J. Fluid Mech. (2004), *vol.* 511, *pp.* 135–178.
DOI: 10.1017/S0022112004009358 Printed in the United Kingdom

An asymptotic theory for the interaction of waves and currents in coastal waters

By JAMES C. McWILLIAMS[1], JUAN M. RESTREPO[2] AND EMILY M. LANE[3]

[1]Department of Atmospheric and Oceanic Sciences and Institute of Geophysics and Planetary Physics, University of California, Los Angeles, CA 90095-1565, USA

[2]Department of Mathematics and Department of Physics, University of Arizona, Tucson, AZ 85721, USA

[3]Program in Applied Mathematics, University of Arizona, Tucson, AZ 85721, USA

(Received 12 March 2003 and in revised form 13 February 2004)

A multi-scale asymptotic theory is derived for the evolution and interaction of currents and surface gravity waves in water of finite depth, under conditions typical of coastal shelf waters outside the surf zone. The theory provides a practical and useful model with which wave–current coupling may be explored without the necessity of resolving features of the flow on space and time scales of the primary gravity-wave oscillations. The essential nature of the dynamical interaction is currents modulating the slowly evolving phase of the wave field and waves providing both phase-averaged forcing of long infra-gravity waves and wave-averaged vortex and Bernoulli-head forces and hydrostatic static set-up for the low-frequency current and sea-level evolution equations. Analogous relations are derived for wave-averaged material tracers and density stratification that include advection by horizontal Stokes drift and by a vertical Stokes pseudo-velocity that is the incompressible companion to the horizontal Stokes velocity. Illustrative solutions are analysed for the special case of depth-independent currents and tracers associated with an incident surface wave field and a vortex with $O(1)$ Rossby number above continental shelf topography.

1. Introduction

We derive approximate dynamical equations for surface gravity waves and currents in a fluid bounded below by a spatially variable bottom topography. The purpose of our modelling differs from well-established theory for effects of topography, nonlinearity, and currents on wave evolution (see Mei 1989 for a review). We focus on how the primary gravity waves (i.e. characteristic of the peak of the wave spectrum) influence currents and vice versa on the longer space and time scales that characterize their nonlinear evolution, with the goal of obtaining a wave-averaged asymptotic model for the mutual interaction of waves and currents in oceanic shelf regions. We accomplish this through the assumption of scale separation between the waves and currents and time averaging over the wave scales. This approach is an extension of McWilliams & Restrepo (1999), but here we do not assume that waves are distinguished from currents entirely by their irrotationality. Rather the distinction between what we mean by waves and currents is made by scale dependences alone; the temporal scale separation is the most fundamental one. The resulting model has the appealing theoretical and practical attribute of making

the large-scale interaction between waves and currents explicit without the burden of resolving the wave oscillations. Our hope is that this model will be useful for discovering new phenomena that arise through wave–current interactions as well as for realistic coastal simulation modelling. We leave open *pro tem* several possible generalizations of the theory of the wave evolution along previously established lines (e.g. dissipation effects).

The ingredients of the dynamics are the following:

(i) Surface gravity waves that (*a*) are approximately irrotational; (*b*) are in water of finite depth (i.e. $\mu = k_0 H_0 \sim 1$, where k_0^{-1} and H_0 are characteristic values for the horizontal scale of the waves and depth of the layer, respectively); (*c*) have a small but finite amplitude (i.e. $\epsilon = a_0 k_0 \ll 1$, where a_0 is a characteristic sea level amplitude for the waves); and (*d*) propagate in a slowly varying environment provided by the topography, long waves, and currents (i.e. with a ratio $\beta \ll 1$ between the characteristic wave and topography/long-wave/current horizontal scales).

(ii) A separate long surface gravity wave component (i.e. an infra-gravity wave), forced by a nonlinear, phase-averaged pressure head and a mass-flux divergence due to the primary waves.

(iii) Nonlinear, rotational currents, whose evolution is influenced by Stokes-drift advection and vortex forces (cf. Craik & Leibovich 1976; McWilliams & Restrepo 1999), as well as other wave-averaged effects.

The theory describes the interactions among these components. It also includes their consequences for material tracers and density stratification.

Work on the interactions among water waves and currents spans nearly half a century. Mainly driven by military, shipping, and shoreline interests, most of the research has focused on how wave nonlinearities affect the shape and spectrum of the waves and on how strong currents affect waves, rather than the other way around. Longuet-Higgins & Stewart (1960, 1961) analyse the nonlinear interaction between short waves and long waves (or currents) and show that variations in the energy of the short waves corresponds to work done by the long waves against the radiation stress of the short waves. In a shoaling area these radiation stresses lead to what are known as the wave set-up and set-down, surf beats, the generation of smaller waves by longer waves, and the steepening of waves on adverse currents and tidal streams (Longuet-Higgins & Stewart 1962, 1964). In Longuet-Higgins (1970) the divergence of this radiation stress is shown to generate an along-shore current by obliquely incident waves on a beach. Peregrine (1976) and Peregrine & Thomas (1979) contribute to the general asymptotic theory on the effects of currents on waves. Thomas (1981, 1990) further investigates the problem both numerically and experimentally. Burrows & Hedges (1985) describe the influence of currents on the oceanic wave climatology. Yoon & Liu (1989) develop a nonlinear dispersive-wave model with current terms. Reviews of wave–wave and wave–current interactions appear in Fenton (1990) and Jonsson (1990).

The effect of waves on currents has been studied much less. It is well known that waves produce a residual Lagrangian current on time and space scales larger than those typical of the waves. Its asymptotic expression is known as the Stokes drift velocity (Longuet-Higgins 1953; Restrepo & Leaf 2002). The coupling of the vorticity in a current with the Stokes drift, known as the vortex force, can lead to a destabilization of the current, forming cells that have striking similarity to oceanic Langmuir circulations (Craik & Leibovich 1976; McWilliams, Sullivan & Moeng 1997). Waves can cause a decrease in tidal-current amplitude with increasing wave height through enhancement of the wave-averaged bottom stress (Grant & Madsen

1979; Prandle 1997; Wolf & Prandle 1999). The wave set-up effect (above) can also be viewed as an effect on the larger scales associated with the currents.

The organization of the paper is the following: the primitive dynamics and non-dimensionalization are defined in § 2; the leading-order wave solution is presented in § 3; the multi-scale asymptotic expansion is defined in § 4; the wave dynamics are more fully determined in §§ 5–7 and Appendices A and C; the forced long-wave dynamics are in § 6 and Appendix B; the current dynamics are in §§ 8–9; the evolution of a material tracer field is in § 10; the generalization to density stratification is in § 11; the classical shallow-water ansatz is derived in § 12, and some of its illustrative solutions are analysed in § 13; and a summary and discussion are in § 14. Appendix D summarizes the definition of the symbols employed.

2. Primitive dynamics

Our starting point is the conservative system of equations for three-dimensional velocity $\boldsymbol{U}(\boldsymbol{x}, z, t)$, sea level $z = E(\boldsymbol{x}, t)$, and material concentration $C(\boldsymbol{x}, z, t)$ in a rotating, finite-depth layer with uniform density ρ_0, a free upper surface of constant pressure, and variable resting depth $z = -H(\boldsymbol{x})$. Here $\boldsymbol{x}$ are the horizontal spatial coordinates and z the vertical one, parallel to gravity, with an upward unit vector $\hat{\boldsymbol{z}}$; $z = 0$ coincides with the quiescent oceanic sea level. We make all equations and variables non-dimensional with a characteristic gravity-wave frequency σ_0 and wavenumber k_0, wave amplitude in sea level a_0, and the linear dispersion relation with a characteristic water depth $H_0 = \mu k_0^{-1}$ (namely $\sigma_0^2 = g k_0 \tanh[\mu]$, where g is the gravitational acceleration and $\mu = k_0 H_0$). Thus, we non-dimensionalize with k_0^{-1} for distance and depth, σ_0^{-1} for time, $a_0 = \epsilon k_0^{-1}$ for E (where $\epsilon = a_0 k_0$), $\epsilon \sigma_0 k_0^{-1}$ for $\boldsymbol{U}$, $\epsilon \rho_0 \sigma_0^2 k_0^{-2}$ for pressure P, and $\epsilon \sigma_0$ for the vorticity $\boldsymbol{\Omega}$. We use f_0 as the scale for the Coriolis frequency, and define a non-dimensional frequency, $f^{nd} = f_0/\sigma_0$, which is equivalent to a Rossby number based on time scales. For convenience, we define the gradient operator in terms of its horizontal and vertical components so that $\nabla \equiv (\nabla_x, \partial/\partial z)$. We similarly write the velocity $\boldsymbol{U} \equiv (\boldsymbol{Q}, W)$. The horizontal extent of the oceanic region of interest is denoted by $\mathscr{D}$ with a boundary $\partial\mathscr{D}$.

The resulting non-dimensional equations of motion are

$$\left.\begin{aligned} &\frac{\partial \boldsymbol{U}}{\partial t} + \epsilon \boldsymbol{U} \cdot \nabla \boldsymbol{U} + f^{nd} \hat{\boldsymbol{z}} \times \boldsymbol{U} + \nabla P + \frac{\hat{\boldsymbol{z}}}{\epsilon \tanh[\mu]} = 0, \\ &\nabla \cdot \boldsymbol{U} = 0, \end{aligned}\right\} \tag{2.1}$$

with a bottom boundary condition of no flow through the ground,

$$W = -\mu \boldsymbol{Q} \cdot \nabla_x H \quad \text{at } z = -\mu H, \tag{2.2}$$

and kinematic and pressure-continuity boundary conditions at the sea surface,

$$\left.\begin{aligned} W &= \frac{\partial E}{\partial t} + \epsilon \boldsymbol{Q} \cdot \nabla_x E, \\ P &= P_0 \quad \text{at } z = \epsilon E. \end{aligned}\right\} \tag{2.3}$$

Here the resting depth H is assumed to be changing appreciably only over large spatial distances. P_0 represents the large-scale atmospheric pressure anomaly from climatology that we assume does not vary spatially on the oceanic scales of interest. We can absorb the gravitational force and surface pressure by defining

$$p = P + \frac{z}{\epsilon \tanh[\mu]} - P_0; \tag{2.4}$$

thus, the final two force terms are replaced by ∇p and the final surface boundary condition by

$$p = \frac{E}{\tanh[\mu]} \quad \text{at } z = \epsilon E. \tag{2.5}$$

Taking the curl of (2.1), we derive the vorticity equation for $\boldsymbol{\Omega} = \nabla \times \boldsymbol{U}$:

$$\frac{\partial \boldsymbol{\Omega}}{\partial t} + \nabla \times [(\epsilon \boldsymbol{\Omega} + f^{nd}\hat{\boldsymbol{z}}) \times \boldsymbol{U}] \; = \; 0. \tag{2.6}$$

(The governing equations for material tracers and buoyancy are deferred until § 10–11.)

A vertical integral of the continuity equation in (2.1), in combination with the vertical boundary conditions on W in (2.2)–(2.3), yields the local mass conservation law,

$$\frac{\partial E}{\partial t} + \nabla_x \cdot \int_{-\mu H}^{\epsilon E} \boldsymbol{Q} \, \mathrm{d}z' = 0. \tag{2.7}$$

With appropriate lateral boundary conditions on $\partial \mathscr{D}$ this system preserves total mass,

$$\mathscr{M} = \int \int_{\mathscr{D}} (\mu H + \epsilon E) \, \mathrm{d}\boldsymbol{x}', \tag{2.8}$$

and energy,

$$\mathscr{E} = \int \int_{\mathscr{D}} \int_{-\mu H}^{\epsilon E} \left(\tfrac{1}{2} \boldsymbol{U} \cdot \boldsymbol{U} + \frac{z'}{\epsilon^2 \tanh[\mu]} \right) \mathrm{d}z' \, \mathrm{d}\boldsymbol{x}'. \tag{2.9}$$

3. Linear gravity wave solutions

To leading order in ϵ, f^{nd}, and β, and making use of the slow variation assumption on H, a non-dimensional solution of (2.1)–(2.5) is

$$\left.\begin{aligned} E &= a \cos[\boldsymbol{k} \cdot \boldsymbol{x} - \sigma t], \\ \boldsymbol{Q} &= \frac{a\boldsymbol{k}}{\sigma \tanh[\mu]} \frac{\cosh[\mathscr{Z}]}{\cosh[\mathscr{H}]} \cos[\boldsymbol{k} \cdot \boldsymbol{x} - \sigma t], \\ W &= \frac{ak}{\sigma \tanh[\mu]} \frac{\sinh[\mathscr{Z}]}{\cosh[\mathscr{H}]} \sin[\boldsymbol{k} \cdot \boldsymbol{x} - \sigma t]. \end{aligned}\right\} \tag{3.1}$$

a is the sea-level height; $\boldsymbol{k}$ is the horizontal wavenumber vector; k is its modulus; $\mathscr{Z} = k(z + \mu H)$ is a rescaled height; $\mathscr{H} = k\mu H$ is a rescaled water depth; and the local dispersion relation is given by

$$\sigma^2 = k \frac{\tanh[\mathscr{H}]}{\tanh[\mu]}. \tag{3.2}$$

As $\mu \to 0$ (i.e. the wavelength becomes very long compared to the depth), $\sigma^2 \to Hk^2$, and as $\mu \to \infty$ (i.e. deep water), $\sigma^2 \to k$.

The physical setting we have in mind is an inner coastal shelf region with its typical wind waves and swell waves. So, for example, for a wavelength of 100 m, then μ is not small except very near the shore where H is small compared to about 15 m (i.e. less than a few metres depth). In this regime there are several non-conservative near-shore processes that are not modelled here but could be appended later: divergence of wave radiation stress due to wave breaking in the surf zone (Longuet-Higgins 1970), bottom drag, and local wave generation by wind stress.

The velocity in (3.1) may be defined in terms of a velocity potential Φ as

$$\boldsymbol{U} = \nabla\Phi,$$

so that for the solution in (3.1),

$$\Phi = \frac{a}{\sigma \tanh[\mu]} \frac{\cosh[\mathscr{Z}]}{\cosh[\mathscr{H}]} \sin[\boldsymbol{k}\cdot\boldsymbol{x} - \sigma t]. \tag{3.3}$$

The associated pressure field satisfies $p = -\partial\Phi/\partial t$, hence

$$p = \frac{a}{\tanh[\mu]} \frac{\cosh[\mathscr{Z}]}{\cosh[\mathscr{H}]} \cos[\boldsymbol{k}\cdot\boldsymbol{x} - \sigma t]. \tag{3.4}$$

The vorticity to leading order is zero,

$$\boldsymbol{\Omega} \equiv \nabla_x \times \boldsymbol{U} = 0.$$

In the more general circumstances analysed below, we shall preserve this wave behaviour at the shortest space and time scales considered.

Substituting (3.1) into (2.9) and averaging over the oscillations leads to an expression for the mean wave energy, valid to leading order in ϵ,

$$\overline{\mathscr{E}} = \frac{a^2}{2\tanh[\mu]}, \tag{3.5}$$

which is composed of equal contributions from the potential and kinetic components.

4. Multi-scale dependences and the asymptotic expansion form

We denote the non-dimensional wave-scale coordinates by $(\boldsymbol{x}, z, t)$. We assume the waves have a slowly varying 'envelope' dynamics in the horizontal and time coordinates $(\boldsymbol{X}, \tau)$, where $\boldsymbol{X} = \beta\boldsymbol{x}$, $\tau = \beta t$, and $\beta \ll 1$, including a 'long-wave' component that does not oscillate in the wave coordinates $(\boldsymbol{x}, t)$. We assume that the bottom topography varies on the coordinate $\boldsymbol{X}$, while the currents have slow scales of variation in the coordinates $\boldsymbol{X}$ and $T = \gamma t$, with $\gamma \ll \beta \ll 1$. We choose an asymptotic expansion form that decomposes the velocity and surface elevation into wave, long-wave, and current components that have the scale dependences described above. An expansion form that retains (3.1)–(3.3) as a leading-order solution is the following:

$$\left.\begin{aligned}
\boldsymbol{Q} &= \boldsymbol{q}(\boldsymbol{x}, z, t, \boldsymbol{X}, \tau, T, \ldots) + \lambda\boldsymbol{q}^{lw}(z, \boldsymbol{X}, \tau, T, \ldots) + \delta\boldsymbol{v}(z, \boldsymbol{X}, T, \ldots) + \cdots,\\
W &= w(\boldsymbol{x}, z, t, \boldsymbol{X}, \tau, T, \ldots) + \lambda\beta w^{lw}(z, \boldsymbol{X}, \tau, T, \ldots) + \delta\beta w^{c}(z, \boldsymbol{X}, T, \ldots) + \cdots,\\
\boldsymbol{\Omega} &= [(\nabla_x, \partial/\partial z) + \beta\nabla_X + \ldots] \times (\boldsymbol{q}, w)\\
&\quad + \lambda\,[(\beta\nabla_X, \partial/\partial z) + \ldots] \times (\boldsymbol{q}^{lw}, \beta w^{lw}) + \delta\,[(\beta\nabla_X, \partial/\partial z) + \ldots] \times (\boldsymbol{v}, \beta w^{c}) + \cdots\\
&\equiv \boldsymbol{\omega}^{w}(\boldsymbol{x}, z, t, \boldsymbol{X}, \tau, T, \ldots) + \lambda\boldsymbol{\omega}^{lw}(z, \boldsymbol{X}, \tau, T, \ldots) + \delta\boldsymbol{\omega}^{c}(z, \boldsymbol{X}, T, \ldots) + \cdots,\\
E &= \eta(\boldsymbol{x}, t, \boldsymbol{X}, \tau, T, \ldots) + \lambda\eta^{lw}(\boldsymbol{X}, \tau, T, \ldots) + \delta\zeta(\boldsymbol{X}, T, \ldots) + \cdots,\\
p &= p^{w}(\boldsymbol{x}, z, t, \boldsymbol{X}, \tau, T, \ldots) + \lambda p^{lw}(z, \boldsymbol{X}, \tau, T, \ldots) + \delta r(z, \boldsymbol{X}, T, \ldots) + \cdots.
\end{aligned}\right\} \tag{4.1}$$

Here $\lambda, \delta \ll 1$. ∇_X denotes a spatial derivative with respect to the slow horizontal coordinate $\boldsymbol{X}$. The right-hand-side quantities $(\boldsymbol{q}, w, \boldsymbol{\omega}^w, \eta, p^w)$ are for the primary surface waves (evolving on fast horizontal and time scales) that are influenced in their slow coordinate dependences by topography, long waves, and currents; we

further denote the three-dimensional wave velocity by $\boldsymbol{u}=(\boldsymbol{q}, w)$. The quantities $(\boldsymbol{q}^{lw}, w^{lw}, \boldsymbol{\omega}^{lw}, \eta^{lw}, p^{lw})$ are for the long waves that arise from wave-averaged nonlinear interactions among the primary waves, with $\boldsymbol{u}^{lw}=(\boldsymbol{q}^{lw}, \beta w^{lw})$. Finally, $(\boldsymbol{v}, w^c, \boldsymbol{\omega}^c, \zeta, p^c)$ are for the slowly evolving wave-averaged currents that are influenced by wave-induced vortex forces, Stokes-drift advection, etc. The topography also has only a slow spatial dependence, $H=H(\boldsymbol{X})$.

We distinguish waves and currents by a slow averaging operator, denoted by $\langle\,\cdot\,\rangle$, over the $(\boldsymbol{x}, t, \tau)$ dependences in (4.1). This implies that all wave quantities have zero slow average, e.g. $\langle\eta\rangle=\langle\eta^{lw}\rangle=0$. We further define a wave-phase average, denoted by $\overline{(\,\cdot\,)}$, over only the $(\boldsymbol{x}, t)$ dependences, which distinguishes the primary and long waves; e.g. for η in (3.1), $\overline{\eta}=0$ and $\overline{\eta^2}=\frac{1}{2}a^2$, and for η^{lw}, $\langle\eta^{lw}\rangle=0$. We thus distinguish two types of fluctuations about these averages by

$$(\,\cdot\,)'=(\,\cdot\,)-\langle\,\cdot\,\rangle, \qquad (\,\cdot\,)^{\dagger}=\overline{(\,\cdot\,)}-\langle\,\cdot\,\rangle, \tag{4.2}$$

where the dot denotes the operand.

Consistent with non-breaking waves near the peak of their spectrum in the ocean, we assume that $\epsilon\ll 1$. We shall use ϵ as the fundamental expansion parameter of the asymptotic theory. The other scaling parameters $[\beta,\ f^{nd},\ \gamma,\ \delta,\ \lambda]\ll 1$ will be chosen in relation to ϵ to permit particular dynamical balances. We will choose them to obtain both a consistent and general leading-order vorticity equation for the wave-averaged current dynamics with advection, rotation, topography and stratification influences, and a general combination of influences from nonlinearity, topography and the currents for the slowly varying envelope dynamics of the waves. We shall see that the scaling choices that allow this are the following:

$$\beta=\epsilon^2, \quad f^{nd}=\epsilon^4 f, \quad \gamma=\epsilon^4, \quad \delta=\epsilon, \quad \lambda=\epsilon, \tag{4.3}$$

where we assume that $f, \mu\sim\epsilon^0=O(1)$. It will be shown that these choices are consistent in (4.1) with the wave velocity remaining irrotational up to $O(\epsilon^2)$ (§§3, 5 and 7) and with the long-wave and current velocities being entirely horizontal up to $O(\delta\beta)=O(\epsilon^3)$.

A physical characterization of the regime of interest can be made by using a primary surface gravity wavelength of 100 m and a wave amplitude of 1.2 m in water with a depth of 100 m. From the dimensional form of (3.2), the wave period is 8 s. The wave steepness is $\epsilon=0.1$. The slow length scale is $\beta^{-1}=\epsilon^{-2}$ times the wavelength or 10 km; this is comparable to the baroclinic deformation radius in coastal regions. The slow time scale is $\gamma^{-1}=\epsilon^{-4}$ times the period or 1 day; this is comparable both to sub-tidal current advective times and to synoptic atmospheric times over which the wind forcing of the primary waves changes. These slow scales are thus relevant for sub-mesoscale and mesoscale topography and currents on a continental shelf.

5. Wave envelope dynamics

Here we construct a slowly varying weakly nonlinear wave theory for gravity waves in finite-depth water, carrying further the approach in Chu & Mei (1970). The basic strategy is to apply WKB theory (c.f. Keller 1958). To leading order the result coincides with the linear solution in §3. At higher orders it includes effects of wave nonlinearity and vorticity, topographic variations, long waves, and currents. In this section we assume that the long-wave $(\eta^{lw}, \boldsymbol{u}^{lw})(\boldsymbol{X}, z, \tau)$ and current $(\zeta, \boldsymbol{v})(\boldsymbol{X}, z, T)$ quantities are known, in order to determine their influence on the primary wave

evolution. (In subsequent sections we shall derive the evolutionary equations for the long waves and currents.)

5.1. *Governing equations*

Exploiting the properties of the velocity field mentioned at the end of the previous section and the scaling choices (4.3), we write

$$\boldsymbol{U} = \nabla\phi + \epsilon(\boldsymbol{q}^{lw} + \boldsymbol{v}) + \epsilon^2\boldsymbol{u}^{wv} + \epsilon^3\hat{\boldsymbol{z}}(w^{lw} + w^c); \tag{5.1}$$

ϕ is the wave component of the velocity potential Φ, and $\boldsymbol{u}^{wv}$ is the wave velocity associated with wave vorticity (i.e. $\boldsymbol{\omega}^w = \nabla \times \boldsymbol{u}^{wv} \neq 0$). The $\epsilon\delta$ prefactor of the wave vorticity is determined by nonlinear interactions with the currents (demonstrated below).

We obtain simplified governing equations for ϕ by dropping terms of $O(\epsilon^3)$ after making use of the scaling relations in (4.3), $\delta = \epsilon$ and $\beta = \epsilon^2$ in particular. The momentum balance (2.1) can be rewritten as

$$\nabla\left(\frac{\partial\phi}{\partial t} + \frac{\epsilon}{2}(\boldsymbol{U}\cdot\boldsymbol{U}) + p + P_0\right) = -\epsilon^2\left(\frac{\partial\boldsymbol{u}^{wv}}{\partial t} + \left(\frac{\partial\boldsymbol{V}}{\partial z}\frac{\partial\phi}{\partial z},\ -\left[\frac{\partial\boldsymbol{V}}{\partial z}\cdot\nabla_x\phi\right]\right)\right) + O(\epsilon^3), \tag{5.2}$$

where

$$\boldsymbol{V} = \boldsymbol{q}^{lw} + \boldsymbol{v} \tag{5.3}$$

is the phase-averaged horizontal velocity. The neglected terms contain current acceleration, Coriolis force, and other higher-order terms. In order to clearly distinguish the irrotational and rotational components of the wave velocity, we require that the left- and right-hand sides of (5.2) vanish separately to the indicated order. The left-hand side yields a Bernoulli integral,

$$\frac{\partial\phi}{\partial t} + \frac{\epsilon}{2}\boldsymbol{U}\cdot\boldsymbol{U} + p + (P_0 - C_b) = 0 + O(\epsilon^3). \tag{5.4}$$

C_b is an arbitrary function of t that appears due to spatial integration of the momentum equations; it will be specified later (§ 9). The right-hand side of (5.2) yields

$$\frac{\partial\boldsymbol{u}^{wv}}{\partial t} = \left(-\frac{\partial\boldsymbol{V}}{\partial z}\frac{\partial\phi}{\partial z}, \left[\frac{\partial\boldsymbol{V}}{\partial z}\cdot\nabla_x\phi\right]\right) + O(\epsilon). \tag{5.5}$$

Clearly, (5.4) is only valid to the indicated order with the particular, but permissible, choice of $\boldsymbol{u}^{wv}$ in (5.5). In §§ 6–7 we present more complete analyses of the long-wave dynamics and the wave vorticity balance, but for now we proceed with the analysis for ϕ, formally assuming that $\boldsymbol{u}^{wv}$ is otherwise known (i.e. just as for $\boldsymbol{u}^{lw}$, η^{lw}, $\boldsymbol{v}$, and ζ).

Continuity in the pressure field allows us to evaluate (5.4) at the free surface:

$$\frac{1}{\tanh[\mu]}E + \frac{\partial\phi}{\partial t} + \frac{\epsilon}{2}(\boldsymbol{U}\cdot\boldsymbol{U}) = C_b - P_0 + O(\epsilon^3), \qquad z = \epsilon E. \tag{5.6}$$

Its material derivative is

$$\Gamma[\phi] + \epsilon\frac{\partial}{\partial t}(\boldsymbol{U}\cdot\boldsymbol{U}) + \frac{\epsilon^2}{2}(\boldsymbol{U}\cdot\nabla)(\boldsymbol{U}\cdot\boldsymbol{U}) + \frac{\epsilon^2}{\tanh[\mu]}w^{wv} = O(\epsilon^3), \quad z = \epsilon E, \tag{5.7}$$

which is obtained by applying $\partial/\partial t + \epsilon \boldsymbol{U}\cdot\boldsymbol{\nabla}$ to (5.6). The operator Γ is defined as

$$\Gamma \equiv \frac{\partial^2}{\partial t^2} + \frac{1}{\tanh[\mu]}\frac{\partial}{\partial z}. \tag{5.8}$$

The incompressibility relation and kinematic boundary conditions from (2.1)–(2.3) are

$$\nabla^2\phi = -\epsilon^2 \boldsymbol{\nabla}\cdot\boldsymbol{u}^{wv}, \qquad -\mu H < z < \epsilon E, \tag{5.9}$$

$$\frac{\partial\phi}{\partial z} = -\mu\epsilon^2 \nabla_x\phi\cdot\nabla_X H - \epsilon^2 w^{wv} + O(\epsilon^3), \qquad z = -\mu H, \tag{5.10}$$

$$\frac{\partial\phi}{\partial z} = \frac{\partial E}{\partial t} + \epsilon \boldsymbol{U}\cdot\nabla_x E - \epsilon^2 w^{wv} + O(\epsilon^3), \qquad z = \epsilon E, \tag{5.11}$$

Next we expand the free-surface conditions in a Taylor series about the mean sea level, $z = 0$. This is done by applying the operator

$$\begin{aligned}\mathscr{R} &\equiv \exp\left(\epsilon E\frac{\partial}{\partial z}\right) = 1 + \epsilon E\frac{\partial}{\partial z} + \frac{\epsilon^2}{2}E^2\frac{\partial^2}{\partial z^2} + O(\epsilon^3)\\ &= 1 + \epsilon\eta\frac{\partial}{\partial z} + \epsilon^2\left(Z\frac{\partial}{\partial z} + \frac{1}{2}\eta^2\frac{\partial^2}{\partial z^2}\right) + O(\epsilon^3)\end{aligned} \tag{5.12}$$

to (5.7) and (5.6) and evaluating the resulting equations at $z = 0$. Here

$$Z = \eta^{lw} + \zeta \tag{5.13}$$

is the phase-averaged sea-level elevation. After substituting from (5.1), we obtain

$$\begin{aligned}\mathscr{R}[\Gamma[\phi]] = &-2\epsilon\left(1 + \epsilon\eta\frac{\partial}{\partial z}\right)\left[\nabla\phi\cdot\nabla\frac{\partial\phi}{\partial t}\right] + \frac{\epsilon^2}{\tan h[\mu]}w^{wv}\\ &- \epsilon^2\left(\frac{1}{2}(\nabla\phi\cdot\nabla)(\nabla\phi\cdot\nabla\phi) + 2\boldsymbol{V}\cdot\nabla_x\frac{\partial\phi}{\partial t}\right) + O(\epsilon^3), \quad z = 0,\end{aligned} \tag{5.14}$$

$$\begin{aligned}\frac{1}{\tanh[\mu]}(\eta + \epsilon Z) = &-\mathscr{R}\left[\frac{\partial\phi}{\partial t}\right] - \frac{\epsilon}{2}\left(1 + \epsilon\eta\frac{\partial}{\partial z}\right)[\nabla\phi\cdot\nabla\phi]\\ &- \epsilon^2(\boldsymbol{V}\cdot\nabla_x\phi) + (C_b - P_0) + O(\epsilon^3), \quad z = 0.\end{aligned} \tag{5.15}$$

The equations (5.9), (5.10), and (5.14) comprise the governing equations for the wave dynamics in ϕ, and (5.15) may be used to evaluate η from ϕ. These differ from those of Chu & Mei (1970) most substantially by including contributions from the wave vorticity (5.5) that, as we shall see, carry significant information about the effects of currents.

5.2. *Wave phase dynamics*

We expand the solution in ϵ,

$$\left.\begin{aligned}\phi &= \phi_0 + \epsilon\phi_1 + \epsilon^2\phi_2 + \cdots,\\ \eta &= \eta_0 + \epsilon\eta_1 + \epsilon^2\eta_2 + \cdots.\end{aligned}\right\} \tag{5.16}$$

At leading order we use a WKB representation for the linear wave solution (3.1) and (3.3) over slowly varying depth, $H(\boldsymbol{X})$,

$$\left.\begin{aligned}\phi_0 &= \tfrac{1}{2}\phi_{01}(\boldsymbol{X}, z, \tau)\mathrm{e}^{\mathrm{i}S(\boldsymbol{X},\tau)/\epsilon^2} + \text{c.c.},\\ \eta_0 &= \tfrac{1}{2}\eta_{01}(\boldsymbol{X}, \tau)\mathrm{e}^{\mathrm{i}S(\boldsymbol{X},\tau)/\epsilon^2} + \text{c.c.},\end{aligned}\right\} \tag{5.17}$$

where

$$\eta_{01} = A(\boldsymbol{X}, \tau), \quad \phi_{01} = -\frac{\mathrm{i}A}{\sigma \tanh[\mu]} \frac{\cosh[\mathscr{Z}]}{\cosh[\mathscr{H}]}. \tag{5.18}$$

Here $\mathrm{i} = \sqrt{-1}$, and c.c. denotes the complex conjugate; ϕ_{01} and η_{01} are complex functions. A is the wave amplitude function in the surface elevation, and S is the phase function that, when divided by ϵ^2 in the exponential, yields oscillations over the fast coordinates $(\boldsymbol{x}, t)$. S is related to the wavenumber vector and frequency by

$$\boldsymbol{k} = \nabla_X S, \quad \sigma = -\frac{\partial S}{\partial \tau}, \tag{5.19}$$

as is customary in ray theory (Lighthill 1978). This solution form satisfies (5.9), (5.10), and (5.14) at leading order in ϵ when the derivatives $(\nabla_x, \partial/\partial t)$ are interpreted as ϵ^2 $(\nabla_X, \partial/\partial\tau)$ when applied to the solution form (5.17) and when the dispersion relation (3.2) holds; i.e.

$$\sigma^2 = \Sigma^2(\boldsymbol{X}, \tau, \boldsymbol{k}) \equiv k \frac{\tanh[\mathscr{H}(\boldsymbol{X}, k)]}{\tanh[\mu]}. \tag{5.20}$$

The accompanying fields for the leading-order wave solution have the following harmonic coefficients in expansion forms analogous to (5.16)–(5.17):

$$\left.\begin{aligned} \boldsymbol{q}_{01} &= \mathrm{i}\boldsymbol{k}\phi_{01} = \frac{A\sigma\boldsymbol{k}}{k \sinh[\mathscr{H}]} \cosh[\mathscr{Z}], \\ w_{01} &= \frac{\partial \phi_{01}}{\partial z} = -\frac{\mathrm{i}A\sigma}{\sinh[\mathscr{H}]} \sinh[\mathscr{Z}], \\ p^w_{01} &= \mathrm{i}\sigma\phi_{01} = \frac{A}{\tanh[\mu]\cosh[\mathscr{H}]} \cosh[\mathscr{Z}], \\ \boldsymbol{\omega}^w_{01} &= 0. \end{aligned}\right\} \tag{5.21}$$

The so-called ray equations for the phase dynamics are completed by the differential consequences of (5.19) and (5.20), namely

$$\left.\begin{aligned} \frac{\partial \boldsymbol{k}}{\partial \tau} + \boldsymbol{C}_g \cdot \nabla_X \boldsymbol{k} &= -\nabla_X \Sigma|_{\tau,\boldsymbol{k}} = -\frac{k\sigma}{\sinh[2\mathscr{H}]} \nabla_X[\mu H], \\ \frac{\partial \sigma}{\partial \tau} + \boldsymbol{C}_g \cdot \nabla_X \sigma &= \left.\frac{\partial \Sigma}{\partial \tau}\right|_{\boldsymbol{x},\boldsymbol{k}} = 0, \end{aligned}\right\} \tag{5.22}$$

where $\boldsymbol{C}_g$ is the group velocity,

$$\boldsymbol{C}_g = \frac{\partial \Sigma}{\partial \boldsymbol{k}} = \frac{\sigma}{2k^2} \left(1 + \frac{2\mathscr{H}}{\sinh[2\mathscr{H}]}\right) \boldsymbol{k}. \tag{5.23}$$

Thus, the leading-order wave solution is wholly determined by the preceding relations except for the slowly varying amplitude A.

5.3. *Wave amplitude dynamics*

To determine A we must consider higher-order dynamical balances. Because of the nonlinearities in (5.14)–(5.15), the wave solution form (5.17) induces other harmonics of the primary oscillation. As in Chu & Mei (1970), we assume that

$$\phi_n = \sum_{m=1}^{n+1} \left(\tfrac{1}{2}\phi_{nm} \mathrm{e}^{\mathrm{i}mS/\epsilon^2} + \text{c.c.}\right), \quad \eta_n = \sum_{m=1}^{n+1} \left(\tfrac{1}{2}\eta_{nm} \mathrm{e}^{\mathrm{i}mS/\epsilon^2} + \text{c.c.}\right) \tag{5.24}$$

for $n \geqslant 1$. Here ϕ_{nm} and η_{nm} are complex functions of the slow variables $(\boldsymbol{X}, \tau)$.

Substituting (5.24) into (5.9), (5.10), and (5.14), then collecting the leading-order linear operator terms on the left-hand sides, yields the following boundary-value problem for ϕ_{nm}:

$$\left(\frac{\partial^2}{\partial z^2} - m^2k^2\right)\phi_{nm} = F_{nm}, \qquad -\mu H < z < 0, \tag{5.25}$$

$$\frac{\partial \phi_{nm}}{\partial z} = B_{nm}, \qquad z = -\mu H, \tag{5.26}$$

$$\left(\frac{1}{\tanh[\mu]}\frac{\partial}{\partial z} - m^2\sigma^2\right)\phi_{nm} = G_{nm}, \qquad z = 0. \tag{5.27}$$

The right-hand sides are functions of solution components with $n' < n$ (in particular, they are trivial for $n = 0$). Similarly, we formally write the η evaluation condition (5.15) as

$$\eta_{nm} - \mathrm{i}m\sigma \tanh[\mu]\phi_{nm} = H_{nm}, \qquad z = 0. \tag{5.28}$$

When F_{n1}, B_{n1}, or G_{n1} is non-trivial, there is a compatibility condition that must be satisfied for the solution form (5.17) and (5.24) to be valid. This compatibility condition arises from the Fredholm Alternative Theorem; from the adjoint problem for (5.25)–(5.27), we can derive the following:

$$\int_{-\mu H}^{0} \phi_{01}^* F_{n1}\, \mathrm{d}z' = \tanh[\mu] G_{n1}\phi_{01}^*|_{z=0} - B_{n1}\phi_{01}^*|_{z=-\mu H} \tag{5.29}$$

for all $n \geqslant 1$, where * denotes complex conjugation.

We next apply this condition at $n = 2$ to determine A. This requires that we first evaluate the wave solution at $O(\epsilon)$. Evaluating the right-hand sides of (5.25)–(5.28) from (5.9)–(5.10) and (5.14)–(5.15) with the solution form (5.17), we obtain

$$\left.\begin{aligned} &F_{11} = F_{12} = B_{11} = B_{12} = G_{11} = H_{11} = 0, \\ &G_{12} = \frac{3\mathrm{i}A^2k\sigma}{\tanh[\mu]\sinh[2\mathscr{H}]}, \\ &H_{12} = \frac{A^2k}{2\sinh[2\mathscr{H}]}(\cosh[2\mathscr{H}] - 2). \end{aligned}\right\} \tag{5.30}$$

Given the above the only non-trivial wave components at this order are ϕ_{12} and η_{12}. By solving (5.25)–(5.28) with (5.30), we obtain

$$\left.\begin{aligned} \phi_{12} &= -\frac{3}{8}\frac{\mathrm{i}A^2\sigma}{\sinh^4[\mathscr{H}]}\cosh[2\mathscr{Z}], \\ \eta_{12} &= \frac{A^2k}{2\tanh[\mathscr{H}]}\left(1 + \frac{3}{2\sinh^2[\mathscr{H}]}\right). \end{aligned}\right\} \tag{5.31}$$

At $O(\epsilon^2)$ we evaluate the compatibility condition (5.29) in order to determine A. (We will otherwise evaluate the wave components at $n = 2$ in Appendix A, since they also are needed for later evaluation of wave-averaged forcing of the current equations (§§8–9).) First we evaluate the vortical component of the wave velocity from (5.5)

and (5.18):

$$\left.\begin{aligned} \boldsymbol{q}_0^{wv} &= -\frac{1}{2}\left(\frac{A\sinh[\mathscr{Z}]}{\sinh[\mathscr{H}]}\,\frac{\partial \boldsymbol{V}}{\partial z}\right)\mathrm{e}^{\mathrm{i}S/\epsilon^2} + \text{c.c.},\\ w_0^{wv} &= \frac{1}{2}\left(\frac{\mathrm{i}A\cosh[\mathscr{Z}]}{k\sinh[\mathscr{H}]}\,\boldsymbol{k}\cdot\frac{\partial \boldsymbol{V}}{\partial z}\right)\mathrm{e}^{\mathrm{i}S/\epsilon^2} + \text{c.c.} \end{aligned}\right\} \tag{5.32}$$

Next, using the lower-order solution components (5.18) and (5.31), we evaluate the requisite right-hand-side quantities from (5.9), (5.10), and (5.14):

$$\left.\begin{aligned} F_{21} =& -\frac{1}{\tanh[\mu]}\left(2\boldsymbol{k}\cdot\nabla_X\left[\frac{A\cosh[\mathscr{Z}]}{\sigma\cosh[\mathscr{H}]}\right]\right)\\ &-\frac{1}{\tanh[\mu]}\left(\left[\frac{A\cosh[\mathscr{Z}]}{\sigma\cosh[\mathscr{H}]}\right](\nabla_X\cdot\boldsymbol{k})\right) - \frac{\mathrm{i}A\cosh[\mathscr{Z}]}{k\sinh[\mathscr{H}]}\frac{\partial^2\mathscr{V}}{\partial z^2}(z)\\ B_{21} =& -\frac{A}{\sigma\tanh[\mu]\cosh[\mathscr{H}]}\boldsymbol{k}\cdot\nabla_X\mu H - \frac{\mathrm{i}A}{k\sinh[\mathscr{H}]}\frac{\partial\mathscr{V}}{\partial z}(-\mu H)\\ G_{21} =& \frac{1}{\tanh[\mu]}\left(2\frac{\partial A}{\partial\tau} - \frac{A}{\sigma}\frac{\partial\sigma}{\partial\tau}\right) + \frac{\mathrm{i}2A}{\tanh[\mu]}\left(\frac{\sigma k}{\sinh[2\mathscr{H}]}Z + \mathscr{V}(0)\right)\\ &-\frac{\mathrm{i}A}{k\tanh[\mu]\tanh(\mathscr{H})}\frac{\partial\mathscr{V}}{\partial z}(0) + \frac{\mathrm{i}M}{\tanh[\mu]}A|A|^2, \end{aligned}\right\} \tag{5.33}$$

where

$$\mathscr{V}(z) = \boldsymbol{k}\cdot\boldsymbol{V}(z)$$

and

$$M = k^2\sigma\left(1 + \frac{1}{\sinh^2[\mathscr{H}]} + \frac{9}{8\sinh^4[\mathscr{H}]}\right). \tag{5.34}$$

Inserting (5.33) into the compatibility condition yields an equation for the complex amplitude A:

$$\frac{\partial A}{\partial\tau} + \boldsymbol{C}_g\cdot\nabla_X A + \tfrac{1}{2}A\nabla_X\cdot\boldsymbol{C}_g + \tfrac{1}{2}\mathrm{i}M|A|^2A + \frac{\mathrm{i}kA}{\sinh[2\mathscr{H}]}\left(\sigma Z + 2\int_{-\mu H}^{0}\cosh[2\mathscr{Z}]\mathscr{V}(z)\,\mathrm{d}z\right) = 0. \tag{5.35}$$

This may be more readily interpreted by decomposing A into its magnitude and slow phase,

$$A(\boldsymbol{X},\tau) \equiv |A|\mathrm{e}^{\mathrm{i}\Theta}. \tag{5.36}$$

The equation for the former takes the form of wave action conservation:

$$\frac{\partial\mathscr{A}}{\partial\tau} + \nabla_X\cdot(\boldsymbol{C}_g\mathscr{A}) = 0. \tag{5.37}$$

The action is defined in the usual way as mean wave energy over the intrinsic frequency (Lighthill 1978),

$$\mathscr{A} = \frac{|A|^2}{2\sigma\tanh[\mu]} = \frac{\overline{\mathscr{E}}}{\sigma} \tag{5.38}$$

(cf. (3.5)). Notice that the action evolution does not depend on the long waves, currents, or wave nonlinearity. In contrast, the evolution of the slow phase is

governed by

$$\frac{\partial \Theta}{\partial \tau} + \boldsymbol{C}_g \cdot \nabla_X \Theta + \frac{M}{2}|A|^2 + \frac{k}{\sinh[2\mathscr{H}]}\left(\sigma Z + 2\int_{-\mu H}^{0} \cosh[2\mathscr{Z}]\mathscr{V}(z)\,\mathrm{d}z\right) = 0, \quad (5.39)$$

indicating how the long waves, currents, and wave nonlinearity each induce changes along ray paths. In particular, note that the long waves and currents enter together in a simple additive fashion in the primary wave dynamics. The equation (5.35) for A, which underlies (5.37) and (5.39), has a cubic nonlinearity as previously derived for dispersive surface gravity waves (e.g. Mei 1989, Chap. 12). We shall see in §§6 and 9 that the effects of Z in (5.35) are a combination of cubic nonlinearities, augmenting the explicit nonlinear term, and a variable environment provided by an inverse-barometer response to atmospheric pressure variations. The final term in (5.39) is recognizable as a Doppler shifting of the slowly varying frequency, $-\partial\Theta/\partial\tau$, by a wave-profile weighted-average of the long-wave and current horizontal velocity, $\boldsymbol{V}$. This Doppler shift can be rewritten as

$$\frac{1}{\mathscr{A}}\int_{-\mu H}^{0} \boldsymbol{v}^{St}(z)\cdot\boldsymbol{V}(z)\,\mathrm{d}z\,, \quad (5.40)$$

where $\mathscr{A}$ is the wave action (5.38) and $\boldsymbol{v}^{St}$ is the Stokes drift velocity discussed in §8; in the special case where $\boldsymbol{V}$ is independent of depth (c.f. §12), the profile-weighted Doppler shift is simply $\mathscr{V} = \boldsymbol{k}\cdot\boldsymbol{V}$. Missing from (5.35)–(5.39) are second-order spatial derivatives (e.g. as in a nonlinear Schrödinger amplitude equation; Mei 1989, p. 616) that would act to spread the distribution of A and allow the occurrence of a side-band instability (Benjamin 1967); this effect would be relevant for a shorter wave packet, but in our scaling it is deferred to higher order in ϵ. If desired for the purpose of phenomenological realism, these second-order terms could be appended to (5.35) without asymptotic inconsistency, though in excess of a minimal consistency.

This completes the determination of the wave envelope dynamics to leading order in ϵ and on evolutionary scales to $(\boldsymbol{X}, \tau)$; the dependence on T is implicit in ζ and $\boldsymbol{v}$ in these wave balances.

5.4. *Special limits*

It is worth noting two situations that allow substantial simplification of the wave formulae, as well as those below for the wave-averaged effects on the long waves and currents.

First, in deep water we can smoothly take the limit in the preceding relations as μ and $\mathscr{H} = k\mu H$ become very large. As a consequence, $\sigma \approx \pm\sqrt{k}$,

$$\sinh[\mathscr{H}],\ \cosh[\mathscr{H}] \approx \tfrac{1}{2}\mathrm{e}^{\mathscr{H}},$$

and in the upper ocean,

$$\sinh[\mathscr{Z}],\ \cosh[\mathscr{Z}] \approx \tfrac{1}{2}\mathrm{e}^{\mathscr{H}}\mathrm{e}^{kz}.$$

Commonly these $\mathscr{H}$ and $\mathscr{Z}$ functions appear as denominators and numerators, respectively; thus their ratio has the simple exponential form, e^{kz}. (In contrast, we cannot smoothly take the shallow-water limit on the scale of the primary waves, $\mu, \mathscr{H} \to 0$, since the nonlinear interaction hierarchy for the waves becomes ill-ordered.)

Second, given steady-state boundary conditions for the primary wave field, after adjustment from arbitrary initial conditions it will equilibrate through propagation so that $\partial_\tau = (\cdot)^\dagger = 0$. Under these conditions the forced long-wave component disappears

(§ 6), and the wave envelope dynamics are diagnostically determined from the currents, topography, and boundary conditions, with an implicit evolution only on the time scale T.

6. Long-wave dynamics

In the presence of the primary waves in § 5, there are forcings of long waves (sometimes called infra-gravity waves, to indicate their lower frequency) and currents due to non-trivial wave averages of the nonlinear terms in (2.1) and (2.3). Here we consider this long-wave dynamics, deferring the currents until §§ 8–9. We therefore focus on the response to the averaging operator $(\cdot)^\dagger$ defined in (4.2).

6.1. *Leading-order balances*

Given the coordinate and amplitude dependences in (4.1) and the primitive dynamics of § 2, the leading-order long-wave balances are the following:

$$\frac{\partial \boldsymbol{q}^{lw}}{\partial \tau} + \nabla_X p^{lw} = -\nabla_X \tfrac{1}{2}\big(\boldsymbol{u}_0^2\big)^\dagger, \tag{6.1a}$$

$$\frac{\partial p^{lw}}{\partial z} = -\frac{\partial}{\partial z}\tfrac{1}{2}\big(\boldsymbol{u}_0^2\big)^\dagger, \tag{6.1b}$$

$$\nabla_X \cdot \boldsymbol{q}^{lw} + \frac{\partial w^{lw}}{\partial z} = 0, \tag{6.1c}$$

$$w^{lw}(-\mu H) + \boldsymbol{q}^{lw}(-\mu H)\cdot \nabla_X[\mu H] = 0, \tag{6.1d}$$

$$w^{lw}(0) - \frac{\partial \eta^{lw}}{\partial \tau} = \nabla_X \cdot (\eta_0 \boldsymbol{q}_0(0))^\dagger, \tag{6.1e}$$

$$p^{lw}(0) - \frac{1}{\tanh[\mu]}\eta^{lw} = -\left(\eta_0 \frac{\partial p_0^w}{\partial z}(0)\right)^\dagger. \tag{6.1f}$$

Balances (6.1*b*) and (6.1*f*) occur at $O(\epsilon)$, while the rest occur at $O(\epsilon^3)$; the corrections to (6.1) occur at $O(\epsilon^2)$. The horizontal momentum equation and the kinematic condition at the surface (i.e. (6.1*a*) and (6.1*e*) formally have more contributing right-hand-side terms than the ones listed. Appendix B explains how the listed terms are the non-trivial leading-order contributions. This is an entirely linear long-wave dynamics, forced by the right-hand-side wave-averaged terms.

From (5.21), we can evaluate the long-wave forcing quantities in (6.1) as

$$\left.\begin{aligned} \tfrac{1}{2}\big(\boldsymbol{u}_0^2\big)^\dagger &= \frac{1}{2\tanh[\mu]}\left(\frac{|A|^2 k}{\sinh[2\mathscr{H}]}\cosh[2\mathscr{Z}]\right)^\dagger, \\ (\eta_0 \boldsymbol{q}_0(0))^\dagger &= \frac{1}{2}\left(\frac{|A|^2\sigma \boldsymbol{k}}{k\tanh[\mathscr{H}]}\right)^\dagger \equiv (\boldsymbol{T}^{St})^\dagger, \\ \left(\eta_0 \frac{\partial p_0^w}{\partial z}(0)\right)^\dagger &= \frac{1}{2\tanh[\mu]}\left(|A|^2 k \tanh[\mathscr{H}]\right)^\dagger. \end{aligned}\right\} \tag{6.2}$$

We defer the interpretation of these wave-averaged forcings to §§ 8–9 where they again arise in the current dynamics but with the alternative averaging operator $\langle\cdot\rangle$. But, to connect with other wave-averaged effects on currents, we remark here that the quantity $\boldsymbol{T}^{St}$ is the depth-integrated horizontal transport by the Stokes drift (9.13).

6.2. *Quasi-static sea level and pressure*

We simplify (6.1) by separating out a quasi-static component of the long-wave solution defined by

$$\left.\begin{aligned} \hat{p}^{lw}(z) &\equiv -\tfrac{1}{2}\left(\boldsymbol{u}_0^2(z)\right)^\dagger = -\frac{1}{2\tanh[\mu]}\left(\frac{|A|^2 k}{\sinh[2\mathscr{H}]}\cosh[2\mathscr{Z}]\right)^\dagger, \\ \hat{\eta}^{lw} &\equiv \tanh[\mu]\left[\hat{p}^{lw}(0) + \left(\eta_0 \frac{\partial p_0^w}{\partial z}(0)\right)^\dagger\right] = -\frac{1}{2}\left(\frac{|A|^2 k}{\sinh[2\mathscr{H}]}\right)^\dagger. \end{aligned}\right\} \tag{6.3}$$

These relations (and their slow-averaged counterparts in §9.2) express the 'set-up' phenomenon (Longuet-Higgins & Stewart 1962, 1964), whereby the mean sea level is more depressed under larger-amplitude waves. Furthermore, $\hat{\eta}^{lw}$ contributes, through the term containing Z, to the nonlinear influence on the slow phase evolution of the primary waves by augmenting the $|A|^2$ coefficient M in (5.39).

6.3. *Long-wave currents*

We denote the residual components of (p^{lw}, η^{lw}) by $(\tilde{p}^{lw}, \tilde{\eta}^{lw})$:

$$p^{lw} = \hat{p}^{lw} + \tilde{p}^{lw}, \qquad \eta^{lw} = \hat{\eta}^{lw} + \tilde{\eta}^{lw}. \tag{6.4}$$

The latter components are in dynamical balance with non-zero $\boldsymbol{q}^{lw}$ and w^{lw}.

After subtracting the quasi-static balances, (6.1*a*) implies that $\boldsymbol{q}^{lw}$ is vertically irrotational; hence, we can define a long-wave horizontal velocity potential,

$$\boldsymbol{q}^{lw} = \nabla_X \varphi^{lw}. \tag{6.5}$$

Relation (6.1*b*) implies that

$$\frac{\partial \tilde{p}^{lw}}{\partial z} = \frac{\partial \boldsymbol{q}^{lw}}{\partial z} = \frac{\partial \varphi^{lw}}{\partial z} = 0; \tag{6.6}$$

hence this long-wave component satisfies a classical shallow-water dynamics with w^{lw} a linear function of z. Eliminating $\tilde{p}^{lw}$ and w^{lw} in (6.1) and noting that

$$\frac{\partial \varphi^{lw}}{\partial \tau} = -\frac{1}{\tanh[\mu]}\tilde{\eta}^{lw}, \tag{6.7}$$

we obtain a forced horizontal wave equation for the long-wave velocity potential,

$$\frac{\partial^2 \varphi^{lw}}{\partial \tau^2} - \nabla_X \cdot [(C^{lw})^2 \nabla_X \varphi^{lw}] \;=\; \mathscr{F}^{lw}, \tag{6.8}$$

where

$$C^{lw} = \sqrt{\frac{\mu H}{\tanh[\mu]}} \tag{6.9}$$

is the long (i.e. non-rotating, shallow-water) gravity-wave speed and the wave-averaged forcing is

$$\begin{aligned} \tilde{\mathscr{F}}^{lw} &= \frac{1}{\tanh[\mu]}\left(\nabla_X \cdot (\boldsymbol{T}^{St})^\dagger + \frac{\partial \hat{\eta}^{lw}}{\partial \tau}\right) \\ &= \frac{1}{2\tanh[\mu]}\left[\nabla_X \cdot \left(\frac{|A|^2 \sigma \boldsymbol{k}}{k \tanh[\mathscr{H}]}\right)^\dagger - \frac{\partial}{\partial \tau}\left(\frac{|A|^2 k}{\sinh[2\mathscr{H}]}\right)^\dagger\right]. \end{aligned} \tag{6.10}$$

Equations (6.8)–(6.10) are a two-dimensional variable-depth generalization of the long-wave dynamics in Mei (1989, p. 613). All of $\boldsymbol{q}^{lw}$, $\tilde{\eta}^{lw}$, and $\hat{\eta}^{lw}$ contribute through $\mathscr{V}$ and Z to the nonlinearity in the slow phase evolution (5.39), as functionals of $|A|^2$.

In the special case of deep-water primary waves ($\mu \gg 1$; § 5.4), $\tilde{\eta}^{lw} \ll 1$ in (6.10) (c.f. $\hat{\zeta} \ll 1$ in § 9.2), and the long-wave horizontal velocity may or may not retain its depth-independent structure, depending upon whether $\mu\epsilon^2$ is small or not. In the latter case, the preceding relations must be corrected accordingly. In the case of steady-state primary waves (i.e. $(\cdot)^\dagger = 0$; § 5.4), all of the long-wave forcings in (6.2) vanish, hence so does the necessity for a long wave component due to primary-wave nonlinearity. In this case the only significant wave-averaged forcing is for the currents (§§ 8–9).

6.4. *Long-wave vorticity*

The ordering choices (4.3) and the expansion form (4.1) make it useful both to rescale and to define an anisotropic decomposition of the long-wave vorticity:

$$\epsilon\boldsymbol{\omega}^{lw} = \epsilon\,(\boldsymbol{\xi}^{lw},\ \epsilon^2\chi^{lw}), \tag{6.11}$$

where

$$\boldsymbol{\xi}^{lw} = \hat{\boldsymbol{z}} \times \left(\frac{\partial \boldsymbol{q}^{lw}}{\partial z} - \epsilon^4 \nabla_X w^{lw} \right) \ = \ \hat{\boldsymbol{z}} \times \frac{\partial \boldsymbol{q}^{lw}}{\partial z} + O(\epsilon^4)$$

is a purely horizontal vector and

$$\chi^{lw} = \hat{\boldsymbol{z}} \cdot \nabla_X \times \boldsymbol{q}^{lw}.$$

However, the depth independence of $\boldsymbol{q}^{lw}$ and the vanishing of its vertical component of curl, implied by (6.1*a*) and by (6.5), imply that

$$\boldsymbol{\xi}^{lw},\ \chi^{lw} = O(\epsilon^2). \tag{6.12}$$

This indicates that the long waves are irrotational to a high order. We will see that this is sufficient to ensure that the long-wave component contributes to the primary wave vorticity (§ 7) in only a limited way and not at all to the current vorticity balance (§ 8).

6.5. *A propagating wave packet*

The wave-packet problem is for a primary wave whose amplitude function, A, has compact support and propagates with $\boldsymbol{C}_g$ in (5.23) as described in §§ 5.2–5.3. No current is forced by the wave packet since the average of the wave forcing over the τ scale is trivial. An analytic solution may be obtained for the special circumstances in which H, $\boldsymbol{k}$, and σ are constant, and A is uniform in the direction perpendicular to $\boldsymbol{k}$. In this case the primary wave has uniform steady-state propagation in $(\boldsymbol{X}, \tau)$ for all its dependent variables except Θ. We define a slow horizontal coordinate moving with $\boldsymbol{C}_g$ and parallel to the phase propagation,

$$X_* = \frac{\sigma \boldsymbol{k}}{|\sigma k|} \cdot (\boldsymbol{X} - \boldsymbol{C}_g \tau). \tag{6.13}$$

A steady-state solution to (6.8)–(6.10) is

$$\boldsymbol{q}^{lw}(X, Y, \tau) = \nabla_X \varphi^{lw} = -\left(\frac{(C^{lw})^2}{(C^{lw})^2 - \boldsymbol{C}_g^2} \right) \left(\frac{1}{\mu H} \boldsymbol{T}^{St} + \boldsymbol{C}_g \left[-\frac{\hat{\eta}^{lw}}{\mu H} \right] \right)(X_*). \tag{6.14}$$

From (5.23) and (6.2), $\boldsymbol{T}^{St}$ and $\boldsymbol{C}_g$ are in the same direction and thus combine constructively in (6.14). From (5.23) and (6.9),

$$\frac{|\boldsymbol{C}_g|}{C^{lw}} = \sqrt{\frac{\tanh[\mathscr{H}]}{\mathscr{H}}} \left(\frac{1}{2} + \frac{\mathscr{H}}{\sinh[2\mathscr{H}]}\right) \leqslant 1 \quad \forall \quad \mathscr{H} \geqslant 0. \tag{6.15}$$

This indicates that the forced long-wave horizontal velocity moves with the wave packet; it is uniform perpendicular to X_* (as is the primary wave packet); and it is directed oppositely to $\boldsymbol{T}^{St}/\mu H$ (the depth-averaged Stokes drift; see §§ 8 and 9.3) at a speed that is either equal to it (as $\mathscr{H} \to \infty$; deep water on the primary wave scale) or faster (n.b. $\boldsymbol{T}^{St}$ remains finite while $\hat{\eta}^{lw} \to 0$ as $\mathscr{H} \to \infty$). As $\mathscr{H} \to 0$ (shallow water on the primary wave scale), $|\boldsymbol{q}^{lw}| \to \infty$ since $|\boldsymbol{C}_g| \to C^{lw}$. Since the asymptotic theory here is valid for $\mathscr{H} \sim 1$, alternative analyses should be made for these extreme limits.

This behaviour corresponds to the discussions in McIntyre (1981) and Craik (1985, § 11.2) based on several earlier analyses referenced therein. Although the asymptotic scaling relations in (4.3) differ from those in the previous derivations, the resulting solution is the same. Once the preceding special assumptions are relaxed with more general initial and topographic conditions, we can expect departures from steady-state propagation with non-trivial evolution of the wave packet properties and a 'wake' of long-wave currents forced by the packet as determined from the relations in §§ 5.2–3 and 6.3.

7. Wave vorticity balance

The preceding wave dynamics are irrotational up to the first two leading expansion orders. The first non-trivial wave vorticity arises at $O(\epsilon^2)$ due to the background vorticity provided by the currents, as indicated in (5.5). To evaluate the wave quantities in § 5, only a leading-order approximation to $(\boldsymbol{\xi}^w,\ \chi^w)$ is required; however, to evaluate the averaged wave forcings in the current vorticity balance (§ 8), an approximation to $O(\epsilon^2)$ is needed.

The ordering choices (4.3) and the expansion form (4.1) make it useful both to rescale and to define an anisotropic decomposition for the primary wave and current vorticities (as done for the long wave in (6.11)):

$$\boldsymbol{\omega}^w = \epsilon^2(\boldsymbol{\xi}^w,\ \chi^w), \qquad \epsilon\boldsymbol{\omega}^c = \epsilon\,(\boldsymbol{\xi}^c,\ \epsilon^2\chi^c). \tag{7.1}$$

The $\boldsymbol{\xi}$ are purely horizontal vectors. Thus, based on the ϵ ordering in (5.1) and (7.1),

$$(\boldsymbol{\xi}^w,\ \chi^w) = \nabla \times \boldsymbol{u}^{wv}.$$

Also,

$$\boldsymbol{\xi}^c = \hat{\boldsymbol{z}} \times \left(\frac{\partial \boldsymbol{v}}{\partial z} - \epsilon^4 \nabla_X w^c\right) = \hat{\boldsymbol{z}} \times \frac{\partial \boldsymbol{v}}{\partial z} + O(\epsilon^4). \tag{7.2}$$

Note that the formal scaling of the long-wave and current vorticities is identical, although (6.12) indicates that the former are actually much smaller.

From (2.6) and (4.1), we have

$$\epsilon^{-2}\frac{\partial \boldsymbol{\omega}^w}{\partial t} = -\nabla \times [(\boldsymbol{\omega}^{lw} + \boldsymbol{\omega}^c + \epsilon^2 f\hat{\boldsymbol{z}}) \times \boldsymbol{u}] \\ - \epsilon\nabla \times [(\epsilon^{-2}\boldsymbol{\omega}^w) \times \boldsymbol{u}]' - \epsilon^2\nabla \times [(\epsilon^{-2}\boldsymbol{\omega}^w) \times \boldsymbol{V}] + O(\epsilon^3), \tag{7.3}$$

where $f = \epsilon^{-4} f^{nd}$ is an order-one constant and the prime superscript denotes departure from the wave average (4.2). The solutions to (7.3) for the wave vorticity to $O(\epsilon^2)$ are in Appendix C.

8. Current vorticity balance

The leading-order vorticity balance for currents comes from averaging (2.6) over wave scales. The expansion form in (4.1) and parameter relations in (4.3) have been chosen so that the tendency, advection, and wave-averaged forcing terms all enter at the leading order. Formally, we write this at $O(\epsilon^5)$ as

$$\frac{\partial \boldsymbol{\omega}^c}{\partial T} + \epsilon^{-2}\nabla \times [(\boldsymbol{\omega}^c + \epsilon^2 f \hat{\boldsymbol{z}}) \times (\boldsymbol{v}, \epsilon^2 w^c)] = -\epsilon^{-2}\nabla \times \langle (\epsilon^{-2}\boldsymbol{\omega}^w) \times \boldsymbol{u} \rangle, \tag{8.1}$$

but its leading-order balances are more apparent when we decompose it into horizontal and vertical components at $O(\epsilon^5)$ and $O(\epsilon^7)$, respectively:

$$\left.\begin{aligned} &\frac{\partial \boldsymbol{\xi}^c}{\partial T} + \left(\boldsymbol{v}\cdot\nabla_X + w^c\frac{\partial}{\partial z}\right)\boldsymbol{\xi}^c - \left(\boldsymbol{\xi}^c\cdot\nabla_X + (f+\chi^c)\frac{\partial}{\partial z}\right)\boldsymbol{v} \\ &\quad = +\hat{\boldsymbol{z}} \times \frac{\partial \boldsymbol{J}}{\partial z} - [\hat{\boldsymbol{z}} \times \nabla_X]K, \\ &\frac{\partial \chi^c}{\partial T} + \left(\boldsymbol{v}\cdot\nabla_X + w^c\frac{\partial}{\partial z}\right)(f+\chi^c) - \left(\boldsymbol{\xi}^c\cdot\nabla_X + (f+\chi^c)\frac{\partial}{\partial z}\right)w^c \\ &\quad = \hat{\boldsymbol{z}}\cdot\nabla_X \times \boldsymbol{J}, \end{aligned}\right\} \tag{8.2}$$

where

$$\left.\begin{aligned} &\boldsymbol{\xi}^c = \hat{\boldsymbol{z}} \times \left(\frac{\partial \boldsymbol{v}}{\partial z} - \epsilon^2 \nabla_X w^c\right) \approx \hat{\boldsymbol{z}} \times \frac{\partial \boldsymbol{v}}{\partial z}, \\ &\chi^c = \hat{\boldsymbol{z}}\cdot\nabla_X \times \boldsymbol{v}. \end{aligned}\right\} \tag{8.3}$$

The horizontal vector $\boldsymbol{J}$ is defined by

$$\boldsymbol{J} = \epsilon^{-2}\hat{\boldsymbol{z}} \times \langle w\boldsymbol{\xi}^w - \chi^w \boldsymbol{q} \rangle = \hat{\boldsymbol{z}} \times \left\langle w_0\boldsymbol{\xi}_2^w + w_2\boldsymbol{\xi}_0^w + w_1\boldsymbol{\xi}_1^w - \chi_0^w\boldsymbol{q}_2 - \chi_2^w\boldsymbol{q}_0 - \chi_1^w\boldsymbol{q}_1 \right\rangle, \tag{8.4}$$

and K is defined by

$$K = \hat{\boldsymbol{z}}\cdot\left\langle \boldsymbol{q}_0 \times \boldsymbol{\xi}_0^w \right\rangle. \tag{8.5}$$

The wave-averaged forcing terms in (8.2) come from the right-hand side of (8.1) that has the form of a curl of the so-called wave vortex force, whose horizontal and vertical components, respectively, are $\boldsymbol{J}$ and $\epsilon^{-2}K$ at $O(\epsilon^5)$. These affect the evolution of the current vorticity as a vortex stretching associated with the Stokes drift of material parcels (also see §§9–10). In (8.4), we have used the fact that quadratic products between $n = 0$ and 1 components have zero wave average. We have also used the fact that

$$\left\langle w_0\boldsymbol{\xi}_0^w - \chi_0^w\boldsymbol{q}_0 \right\rangle = 0$$

from (3.1) and (C 6). Since the form of $(\hat{\boldsymbol{\xi}}_2^w, \hat{\chi}_2^w)$ is identical to $(\boldsymbol{\xi}_0^w, \chi_0^w)$ in its dependences upon the primary wave variables, this also implies that the former long-wave terms in (C 8) will make no contribution to $\boldsymbol{J}$ even at $O(1)$, and thus can be ignored for our purposes. The other potential long-wave contributions implicit in the formulae for $(\boldsymbol{\xi}_2^w, \chi_2^w)$ vanish since they enter linearly in $\mathscr{V}$ and disappear after averaging over τ. Finally, there are no vortex forces resulting from averages of quadratic products of long-wave fields (e.g. $\langle \boldsymbol{q}^{lw} \times \boldsymbol{\xi}^{lw} \rangle$) since they would enter (8.2) only at a higher order in ϵ.

We evaluate fully the expressions for $\boldsymbol{J}$ and K from (5.21), (C 6), (C 7), (C 8), (8.4), and (8.5) to obtain the following:

$$\left.\begin{aligned} \boldsymbol{J} &= -\hat{\boldsymbol{z}} \times \langle \boldsymbol{v}^{St} \rangle (\chi^c + f) - \langle w^{St} \rangle \frac{\partial \boldsymbol{v}}{\partial z} - \nabla_X \left[\left\langle \int_{-\mu H}^{z} \boldsymbol{v}^{St}(z')\, \mathrm{d}z' \right\rangle \cdot \frac{\partial \boldsymbol{v}}{\partial z} \right], \\ K &= -\left\langle \int_{-\mu H}^{z} \boldsymbol{v}^{St}(z')\, \mathrm{d}z' \right\rangle \cdot \frac{\partial^2 \boldsymbol{v}}{\partial z^2}. \end{aligned}\right\} \tag{8.6}$$

In both $\boldsymbol{J}$ and K, we note that all the wave-averaged forcing terms are related to the Stokes drift, which is defined and evaluated as

$$\boldsymbol{v}^{St} \equiv \overline{\left[\int^{t} \boldsymbol{u}_0\, \mathrm{d}t \cdot \nabla \right] \boldsymbol{u}_0} = \frac{|A|^2 \sigma}{2 \sinh^2[\mathscr{H}]} \cosh[2\mathscr{Z}] \boldsymbol{k}. \tag{8.7}$$

Its vertical integral is

$$\int_{-\mu H}^{z} \boldsymbol{v}^{St}(z')\, \mathrm{d}z' = \frac{|A|^2 \sigma}{4k \sinh^2[\mathscr{H}]} \sinh[2\mathscr{Z}] \boldsymbol{k}. \tag{8.8}$$

We also have defined a vertical pseudo-velocity,

$$w^{St}(z) = -\nabla_X \cdot \int_{-\mu H}^{z} \boldsymbol{v}^{St}\, \mathrm{d}z'. \tag{8.9}$$

This combines with the horizontal Stokes drift in the following three-dimensional incompressibility relation:

$$\nabla_X \cdot \boldsymbol{v}^{St} + \frac{\partial w^{St}}{\partial z} = 0.$$

We use the term pseudo-velocity here to distinguish it from the vertical component of the averaged quadratic quantity in (8.7) – the true Stokes drift – which is zero. Stokes drift is the Lagrangian mean flow associated with the leading-order wave field, and it has a non-dimensional scaling factor of ϵ (i.e. the same as $\boldsymbol{v}$ in (4.1)).

Since currents are distinguished from waves, not just in their coordinate dependences (4.1), but also in their dominantly vortical, rather than irrotational, character, we can view (8.2) as the central dynamical relations for current evolution under wave influences. However, for a complete characterization of the current fields and their dynamics, we must consider additional relations (§ 9). Further interpretation of the vortex force is in § 9.6.

9. General current balances

Now we examine the wave-averaged continuity and momentum equations and boundary conditions for the currents. In anticipation of the leading-order dynamical balances, we partition the sea level and pressure to isolate a component in static balance with the atmospheric surface pressure and wave field (denoted by $\hat{}$) and a dynamical term (denoted by ^{c}) associated with the currents:

$$\zeta = \hat{\zeta} + \epsilon^2 \zeta^c, \qquad r = \hat{p} + \epsilon^2 p^c. \tag{9.1}$$

The static components are analogous to $(\hat{\eta}^{lw}, \hat{p}^{lw})$ in § 6, except here they are due to the full average over the wave scales.

9.1. *Continuity and bottom boundary condition*

The linear equations are easily averaged. The continuity equation for currents occurs at $O(\epsilon^3)$ compared to (2.1):

$$\nabla_X \cdot \boldsymbol{v} + \frac{\partial w^c}{\partial z} = 0. \tag{9.2}$$

The bottom boundary condition (2.2) also occurs at $O(\epsilon^3)$:

$$w^c = -\mu \boldsymbol{v} \cdot \nabla_X H \quad \text{at } z = -\mu H. \tag{9.3}$$

9.2. *Static pressure and sea-level fields*

The leading-order wave-averaged momentum balance from (2.1) occurs at $O(\epsilon^3)$ horizontally and $O(\epsilon)$ vertically; in both relations it can be integrated spatially to give a balance with the wave kinetic energy density,

$$\hat{p} = -\tfrac{1}{2}\langle \boldsymbol{u}_0^2 \rangle + C_p, \tag{9.4}$$

which is a simple form of the Bernoulli integral (c.f. (5.4)). The right-hand side is often called a Bernoulli head, here due to the wave-averaged kinetic energy. C_p is an integration constant. There are analogous wave-averaged forms of the surface conditions, (2.5) and (5.15), expanded about $z = 0$ (as in § 5) at $O(\epsilon)$:

$$\left.\begin{aligned} \hat{p}(0) + \left\langle \eta_0 \frac{\partial p_0^w}{\partial z}(0) \right\rangle &= \frac{1}{\tanh[\mu]}\hat{\zeta}, \\ -\left\langle \eta_0 \frac{\partial^2 \phi_0}{\partial z \partial t}(0) \right\rangle - \tfrac{1}{2}\langle \boldsymbol{u}_0^2(0) \rangle + \epsilon^{-1}(C_b - P_0) &= \frac{1}{\tanh[\mu]}\hat{\zeta}. \end{aligned}\right\} \tag{9.5}$$

Using the leading-order wave solution in § 3 or 5, we evaluate the leading-order wave kinetic energy density to be

$$\tfrac{1}{2}\langle \boldsymbol{u}_0^2 \rangle = \frac{1}{2\tanh[\mu]} \left\langle \frac{|A|^2 k}{\sinh[2\mathscr{H}]} \cosh[2\mathscr{Z}] \right\rangle, \tag{9.6}$$

and the wave terms in (9.5) to be

$$\left\langle \eta_0 \frac{\partial p_0^w}{\partial z}(0) \right\rangle = -\left\langle \eta_0 \frac{\partial^2 \phi_0}{\partial z \partial t}(0) \right\rangle = \langle w_0^2(0) \rangle = \frac{1}{2\tanh[\mu]} \langle\, |A|^2 k \tanh[\mathscr{H}] \rangle. \tag{9.7}$$

The latter quantity is thus the mean sea-level tendency variance, $\langle (\partial \eta / \partial t)^2 \rangle$. The first relation in (9.5)–(9.7) – among oceanic surface pressure, atmospheric pressure (c.f. (2.4), sea level, and $\langle w^2 \rangle$ – is similar to one derived in McWilliams & Restrepo (1999); it shows that one cannot infer the oceanic surface pressure without correcting for a wave-averaged term (e.g. in altimetric inferences of dynamic pressure). These relations can be manipulated to show that $C_p = \epsilon^{-1}(C_b - P_0)$ and $C_b = 0$ without loss of generality. Thus, the static sea-level and pressure fields are

$$\left.\begin{aligned} \hat{\zeta} &= -\frac{\tanh[\mu]}{\epsilon} P_0 - \frac{1}{2}\left\langle \frac{|A|^2 k}{\sinh[2\mathscr{H}]} \right\rangle, \\ \hat{p}(z) &= -\frac{1}{\epsilon} P_0 - \frac{1}{2\tanh[\mu]} \left\langle \frac{|A|^2 k}{\sinh[2\mathscr{H}]} \cosh[2\mathscr{Z}] \right\rangle. \end{aligned}\right\} \tag{9.8}$$

The wave forcings in each of these expressions are the same as for their long-wave counterparts in (6.2)–(6.3) except for the difference in averaging operators. The first part of $\hat{\zeta}$ is the 'inverse-barometer' response of sea level to an atmospheric pressure

anomaly (presumed to be $O(\epsilon)$ for well-orderedness), and the second part is the wave set-up on the current time scale. As with η^{lw} in § 6, the current-scale sea-level fluctuations provide, through $\hat{\zeta}$ and Z, an additional cubic nonlinearity in the wave-amplitude balance (5.35). The determining relations for $\hat{p}$ and $\hat{\zeta}$ do not involve the current velocity; hence they may be called static balances.

In the deep-water limit (i.e. $\mathscr{H} \to \infty$), (9.8) indicates that $\hat{\zeta} \to 0$ while $\hat{p}(0)$ remains finite. This implies that the wave set-up effect on sea level becomes negligible in deep water. It also implies that the indicated altimetric correction to inferred surface pressure based on (9.5)–(9.7) becomes applicable only to the static pressure, $\hat{p}(0)$, rather than the dynamic pressure, $p^c(0)$, and thus inconsequential for determination of large-scale geostrophic currents in deep water through the cancellation of the static pressure gradient force and the leading-order Bernoulli-head gradient in the momentum equations (see further remarks at the end of § 9.5).

9.3. *Dynamic surface boundary conditions*

With $\hat{p}$ and $\hat{\zeta}$ fully determined, we proceed to the nonlinear, wave-averaged surface boundary conditions at $O(\epsilon^3)$ and horizontal and vertical momentum equations at $O(\epsilon^5)$ and $O(\epsilon^3)$, respectively. The surface pressure condition (2.5) is

$$\frac{1}{\tanh[\mu]}\zeta^c - p^c(0) = \hat{\zeta}\frac{\partial \hat{p}}{\partial z}(0) + \left\langle \eta^{lw}\frac{\partial p^{lw}}{\partial z}(0)\right\rangle + \frac{1}{\tanh[\mu]}\mathscr{P}_0, \tag{9.9}$$

where the wave-averaged forcing term is

$$\begin{aligned}\frac{1}{\tanh[\mu]}\mathscr{P}_0 = {} & \frac{1}{2}\langle \eta_0^2\rangle \frac{\partial^2 \hat{p}}{\partial z^2}(0) + \frac{1}{2}\left\langle \overline{\eta_0^2}\frac{\partial^2 p^{lw}}{\partial z^2}(0)\right\rangle + \left\langle \eta_0 \frac{\partial^2 p_0^w}{\partial z^2}(0)\right\rangle \hat{\zeta} \\ & + \left\langle \overline{\eta_0 \frac{\partial^2 p_0^w}{\partial z^2}(0)\eta^{lw}}\right\rangle + \left\langle \eta_0 \frac{\partial p_2^w}{\partial z}(0) + \eta_2 \frac{\partial p_0^w}{\partial z}(0) + \eta_1 \frac{\partial p_1^w}{\partial z}(0)\right\rangle \\ & + \left\langle \eta_0\eta_1 \frac{\partial^2 p_0^w}{\partial z^2}(0) + \frac{1}{2}\eta_0^2 \frac{\partial^2 p_1^w}{\partial z^2}(0)\right\rangle + \frac{1}{6}\left\langle \eta_0^3 \frac{\partial^3 p_0^w}{\partial z^3}(0)\right\rangle. \end{aligned} \tag{9.10}$$

Other terms formally contribute here at lower order in ϵ, but they drop out after averaging. The evaluation of $\mathscr{P}_0$ is laborious, involving (5.21), (5.31), (5.33), (A 3), (A 4), (A 5), and (A 7); the result is

$$\begin{aligned}\mathscr{P}_0 = {} & \frac{1}{2}\langle |A|^2 k^2 (1 + \tanh^2[\mathscr{H}])(\hat{\zeta} + \eta^{lw})\rangle + \frac{\tanh[\mu]}{4}\left\langle |A|^2 \frac{\partial^2}{\partial z^2}(\hat{p} + p^{lw})(0)\right\rangle \\ & + \frac{1}{2}\left\langle \frac{|A|^2}{\sigma}\left\{ \frac{\tanh[\mathscr{H}]}{\sinh[2\mathscr{H}]}\left(-\frac{\partial \mathscr{V}}{\partial z}(0) + \cosh[2\mathscr{H}]\frac{\partial \mathscr{V}}{\partial z}(-\mu H)\right.\right.\right. \\ & \left.\left.\left. + \int_{-\mu H}^{0} \frac{\partial^2 \mathscr{V}}{\partial z'^2}\cosh[2kz']\,\mathrm{d}z'\right) - 2k\tanh[\mathscr{H}]\mathscr{V}(0)\right\}\right\rangle \\ & + \frac{1}{4}\left\langle \frac{|A|^4 k^3}{\sinh[2\mathscr{H}]\sinh^4[\mathscr{H}]}\left(9 + \tfrac{9}{2}\sinh^2[\mathscr{H}] - 2\sinh^4[\mathscr{H}]\right)\right\rangle. \end{aligned} \tag{9.11}$$

Note that the surface condition (9.9) between dynamic pressure and sea level at this order relevant to the current dynamics is more complicated in its wave-averaged correction than (9.5). As in the long-wave dynamics (§ 6), it is composed of higher-order contributions to the static sea-level and pressure fields in § 9.2 as

well as dynamical pressure forces for the currents (§ 9.5), but we will not make this decomposition explicitly here.

The surface kinematic condition in (2.3), after expansion about $z = 0$ and averaging, becomes

$$w^c(0) = \nabla_X \cdot \langle \eta_0 \boldsymbol{q}_0(0) \rangle, \tag{9.12}$$

where similar considerations are used in this derivation as in its long-wave counterpart in (6.1). This final expression for the wave-averaged forcing of the surface vertical velocity is familiar from McWilliams & Restrepo (1999): it is the ∇_X divergence of

$$\langle \eta_0 \boldsymbol{q}_0(0) \rangle = \frac{1}{2} \left\langle \frac{|A|^2 \sigma \boldsymbol{k}}{k \tanh[\mathscr{H}]} \right\rangle = \left\langle \int_{-\mu H}^{0} \boldsymbol{v}^{St} \, \mathrm{d}z' \right\rangle \equiv \langle \boldsymbol{T}^{St} \rangle, \tag{9.13}$$

the depth-integrated Stokes drift (c.f. (8.7)–(8.8)). This relation is the counterpart of the long-wave $(\eta_0 \boldsymbol{q}_0(0))^{\dagger}$ flux in (6.2).

9.4. *Mass balance*

The depth-integrated Stokes drift also appears in the wave-averaged local mass conservation law from (2.7) at its leading order, $O(\epsilon^3)$: from (9.2)–(9.3) and (9.12),

$$\nabla_X \cdot \int_{-\mu H}^{0} \boldsymbol{v} \, \mathrm{d}z' = -w^c(0) = -\nabla_X \cdot \langle \boldsymbol{T}^{St} \rangle = \langle w^{St}(0) \rangle. \tag{9.14}$$

This indicates that the leading-order horizontal mass transport divergence by the currents is equal and opposite to that by the waves. Equivalently, the current vertical velocity at the surface is equal and opposite to the surface value of the vertical pseudo-velocity w^{St} from (8.9). However, this does not imply an equivalence of mass transport by waves and currents because the rotational component, $\hat{\boldsymbol{z}} \cdot \nabla_X \times \int_{-\mu H}^{0} \boldsymbol{v} \, \mathrm{d}z'$, is unconstrained. For most large-scale currents the rotational component is much larger than the divergent component (e.g. § 13).

9.5. *Momentum balance*

Substituting (4.1) into (2.1) and averaging with $\langle \cdot \rangle$ yields the leading-order horizontal momentum balance for currents at $O(\epsilon^5)$:

$$\frac{\partial \boldsymbol{v}}{\partial T} + \left(\boldsymbol{v} \cdot \nabla_X + w^c \frac{\partial}{\partial z} \right) \boldsymbol{v} + f \hat{\boldsymbol{z}} \times \boldsymbol{v} + \nabla_X p^c = -\nabla_X \mathscr{K} + \boldsymbol{J}. \tag{9.15}$$

The first right-hand-side group of wave-averaged forcing terms here is minus the gradient of the primary- and long-wave horizontal kinetic energy density at $O(\epsilon^2)$, namely a higher-order form of the Bernoulli head,

$$\begin{aligned} \mathscr{K} &= \left\langle \boldsymbol{u}_2 \cdot \boldsymbol{u}_0 + \tfrac{1}{2} \boldsymbol{u}_1^2 + \tfrac{1}{2} (\boldsymbol{q}^{lw})^2 \right\rangle \\ &= \frac{1}{4} \left\langle \frac{\sigma |A|^2}{k \sinh^2[\mathscr{H}]} \left(-\sinh[2\mathscr{Z}] \frac{\partial \mathscr{V}}{\partial z} + \int_{-\mu H}^{z} \frac{\partial^2 \mathscr{V}}{\partial z'^2} \sinh[2k(z - z')] \, \mathrm{d}z' \right) \right\rangle \\ &\quad + \frac{9}{64} \left\langle \frac{|A|^4 \sigma^2 k^2 \cosh[4\mathscr{Z}]}{\sinh^8[\mathscr{H}]} \right\rangle + \tfrac{1}{2} \langle (\boldsymbol{q}^{lw})^2 \rangle, \end{aligned} \tag{9.16}$$

and the second group here is part of the wave vortex force, $\langle \boldsymbol{u} \times \boldsymbol{\omega}^w \rangle$, where $\boldsymbol{J}$ is defined in (8.4). Its curl, of course, leads to (8.2). In (9.16) the explicit evaluation of the long-wave contribution can be done only after solving (6.8), (6.5), and (6.7).

The vertical momentum balance for currents at $O(\epsilon^3)$ is

$$\frac{\partial p^c}{\partial z} = -\frac{\partial \mathscr{K}}{\partial z} + K, \tag{9.17}$$

which has the same types of wave-averaged forcing terms, with K defined in (8.5). This is a quasi-hydrostatic balance since the vertical acceleration and mean advection are negligible.

Because the depth-integrated mass balance (9.14) lacks the tendency term $\partial\zeta/\partial T$, which is smaller than the retained terms by $O(\epsilon^4)$, we must solve a diagnostic relation for p^c in order to time-integrate the current dynamical equations. This relation is obtained by integrating (9.15) over the resting depth interval $(-\mu H, 0)$, taking the horizontal divergence, and using (9.14) to replace the depth-integrated acceleration with a T derivative of the Stokes transport (which is fully determined from the wave's forcing and boundary conditions independently from the current fields). The result is a diagnostic equation for $\nabla_X \cdot \int_{-\mu H}^{0} \nabla_X p^c \, \mathrm{d}z'$ in terms of present values of the current velocity and wave-averaged forcing terms. The complementary vertical variation of p^c is determined from (9.17). With p^c determined, (9.9) is a diagnostic relation for ζ^c.

For radar altimetric inferences of $p^c(0)$ from measurements of ζ^c, the static components, $\hat{p}$ and $\hat{\zeta}$, must first be eliminated as described in § 9.2 (n.b. the elimination is trivial in deep water). As shown above, however, there are other wave-averaged contributions through $\mathscr{P}_0$ in (9.10) and $\mathscr{K}$ in (9.16) that in principle must also be included in this inference; furthermore, some of these contributions involve wave–current products that are unknown *a priori*. Nevertheless, in the limit of small Rossby number for the currents (i.e. $V^c \ll f L^c$, dimensionally), these contributions in $\mathscr{P}_0$ and $\mathscr{K}$ are small compared to the geostrophically balanced components of $p^c(0)$ and ζ^c, and thus this aspect of the altimetric inference remains valid.

In (9.15) the Coriolis forces involving f combine into $-f\hat{\boldsymbol{z}} \times (\boldsymbol{v} + \langle \boldsymbol{v}^{St} \rangle)$, after using (8.6). Ursell (1950) noted that, for rotating flows in the presence of a steady spatially uniform primary wave, the only conservative, steady, uniform current solution is $\boldsymbol{v}(z) = -\langle \boldsymbol{v}^{St} \rangle(z)$ since all other forces vanish. This solution is also consistent with the mass balance (9.14). This has sometimes been misinterpreted as an indication that the wave-averaged effect on currents may be only a trivial cancellation of the Stokes drift, otherwise leaving the currents the same as if there were no waves. In the usual oceanic regimes with non-steadiness and spatial non-uniformity for all quantities, this conclusion is logically unwarranted, and the particular solutions in § 13 demonstrate that the interpretation is often far from valid.

9.6. *Vortex force and Bernoulli head*

The vortex force $\epsilon^5(\boldsymbol{J},\ \epsilon^{-2}K)$ in (8.6) is non-unique in its contribution to the current vorticity balance (8.2) with respect to any irrotational force vector. The Bernoulli head force in (9.15) and (9.17), namely

$$-\epsilon^5 \left(\nabla_X,\ \epsilon^{-2} \frac{\partial}{\partial z} \right) \mathscr{K}, \tag{9.18}$$

is such an irrotational vector. The following three-dimensional vector identity can be

demonstrated:

$$\epsilon^5(\boldsymbol{J}, \epsilon^{-2}K) = \epsilon^5(\langle \boldsymbol{v}^{St}\rangle, \epsilon^2\langle w^{St}\rangle) \times (\epsilon^{-2}\boldsymbol{\xi}^c,\ f+\chi^c) - \epsilon^5\left(\nabla_X, \epsilon^{-2}\frac{\partial}{\partial z}\right)\left[\left\langle \int_{-\mu H}^{z} \boldsymbol{v}^{St}(z')\,\mathrm{d}z' \right\rangle \cdot \frac{\partial \boldsymbol{v}}{\partial z}\right]. \quad (9.19)$$

The left-hand side is the vortex force in (8.6); the first right-hand-side term has the classical vortex-force form of the vector cross-product of Stokes drift and absolute current vorticity (Craik & Leibovich 1976, with $f=0$; McWilliams & Restrepo 1999), here generalized to include the Stokes vertical pseudo-velocity; and the second right-hand-side term is another obviously irrotational force vector.

For the dual reasons of retaining contact with the classical form and of simplifying the evaluation formulae for both quantities, we choose to shift the second right-hand-side term in (9.19) from the vortex force and combine it with the Bernoulli-head force; in doing so the first term in the second line of (9.16) cancels. Thus, we redefine the vortex force and the Bernoulli head (as denoted by an asterisk subscript) to be

$$\left.\begin{aligned} \boldsymbol{J}_* &= -\hat{\boldsymbol{z}} \times \langle \boldsymbol{v}^{St}\rangle(\chi^c + f) - \langle w^{St}\rangle \frac{\partial \boldsymbol{v}}{\partial z}, \\ K_* &= \langle \boldsymbol{v}^{St}\rangle \cdot \frac{\partial \boldsymbol{v}}{\partial z}, \\ \mathscr{K}_* &= \frac{1}{4}\left\langle \frac{\sigma|A|^2}{k\sinh^2[\mathscr{H}]} \int_{-\mu H}^{z} \frac{\partial^2 \mathscr{V}}{\partial z'^2} \sinh[2k(z-z')]\,\mathrm{d}z' \right\rangle \\ &\quad + \frac{9}{64}\left\langle \frac{|A|^4\sigma^2k^2\cosh[4\mathscr{Z}]}{\sinh^8[\mathscr{H}]} \right\rangle + \tfrac{1}{2}\langle (\boldsymbol{q}^{lw})^2\rangle. \end{aligned}\right\} \quad (9.20)$$

The redefined quantities ($\boldsymbol{J}_*,\ K_*,\ \mathscr{K}_*$) can replace ($\boldsymbol{J},\ K,\ \mathscr{K}$) in (8.2), (9.15), (9.17), and all their derivative relations.

In summary, the current fields, ($\boldsymbol{v},\ w^c,\ \boldsymbol{\xi}^c,\ \chi^c, p^c,\ \zeta^c$), are fully determined at their leading orders from (9.15), (9.17), (9.2), (8.2), (9.3), (9.9), and (9.12), once their wave-averaged forcings are determined from the wave dynamics in §§5–7.

10. Material tracers

The non-dimensional primitive equation for conservation of a material tracer is

$$\frac{\partial \mathscr{C}}{\partial t} + \epsilon \boldsymbol{U} \cdot \nabla \mathscr{C} = 0. \quad (10.1)$$

The non-dimensional scale for $\mathscr{C}$ is irrelevant since this equation is linear in $\mathscr{C}$. Analogous to (4.1), we decompose $\mathscr{C}$ into primary- and long-wave and current components,

$$\mathscr{C} = \nu(c(\boldsymbol{x}, z, t, \boldsymbol{X}, \tau, T, \ldots) + \lambda c^{lw}(\boldsymbol{X}, \tau, T, \ldots)) + C(z, \boldsymbol{X}, T, \ldots), \quad (10.2)$$

where $\nu \ll 1$ because c arises at its leading order as a consequence of wave advection of ∇C, specifically the vertical stratification. This is also true for the long-wave component c^{lw}, recalling that $\lambda = \epsilon$ in (4.3). Here the choice $\nu = \epsilon$ leads to the following rapidly fluctuating tracer balance:

$$\frac{\partial c}{\partial t} = -w\frac{\partial C}{\partial z} - \epsilon(\nabla\phi \cdot \nabla c)' - \epsilon^2\left(w\frac{\partial c^{lw}}{\partial z} + \boldsymbol{q} \cdot \nabla_X C + \boldsymbol{V} \cdot \nabla_x c\right) + O(\epsilon^3). \quad (10.3)$$

As with wave vorticity (§ 7 and Appendix C), we can expand c in powers of ϵ and integrate (10.3) over the fast time to obtain

$$\left.\begin{aligned} c_0 &= -\frac{\partial C}{\partial z}\left(\int^t w_0\,\mathrm{d}t\right), \\ c_1 &= -\frac{\partial C}{\partial z}\left(\int^t w_1\,\mathrm{d}t\right) - \int^t (\nabla\phi_0\cdot\nabla c_0)'\,\mathrm{d}t, \\ c_2 &= -\frac{\partial C}{\partial z}\left(\int^t w_2\,\mathrm{d}t\right) - \frac{\partial c^{lw}}{\partial z}\left(\int^t w_0\,\mathrm{d}t\right) - \nabla_X C\cdot\left(\int^t \boldsymbol{q}_0\,\mathrm{d}t\right) \\ &\quad - \boldsymbol{V}\cdot\left(\int^t \nabla_x c_0\,\mathrm{d}t\right) - \int^t (\nabla\phi_0\cdot\nabla c_1 + \nabla\phi_1\cdot\nabla c_0)'\,\mathrm{d}t - \left(\int^t \frac{\partial c_0}{\partial\tau}\,\mathrm{d}t\right). \end{aligned}\right\} \tag{10.4}$$

The slow evolution of C is determined at $O(\epsilon^4)$ by

$$\frac{\partial C}{\partial T} + \left(\boldsymbol{v}\cdot\nabla_X + w^c\frac{\partial}{\partial z}\right)C = -\epsilon^{-2}\langle\,\nabla\cdot\boldsymbol{u}c\rangle, \tag{10.5}$$

where we have used the three-dimensional non-divergence of $\boldsymbol{u}$ to rewrite the right-hand side as a wave-averaged material flux divergence. Again, there are no averaged contributions from products of the long-wave components at this order.

In spite of its appearance, the wave-averaged forcing in (10.5) is actually $O(1)$, as we now show. Expanding the right-hand side to $O(1)$, we obtain

$$\begin{aligned} -\epsilon^{-2}\langle\,\nabla\cdot\boldsymbol{u}c\rangle &= -\nabla_X\cdot\langle\,\boldsymbol{q}_0 c_0\rangle \\ &\quad - \epsilon^{-2}\frac{\partial}{\partial z}\langle w_0 c_0\rangle - \epsilon^{-1}\frac{\partial}{\partial z}\langle w_0 c_1 + w_1 c_0\rangle \\ &\quad - \frac{\partial}{\partial z}\langle\,w_0 c_2 + w_1 c_1 + w_2 c_0\rangle. \end{aligned} \tag{10.6}$$

The middle-line terms vanish: the first one vanishes because $c_0 \propto \int^t w_0\,\mathrm{d}t$ and the resulting $\langle w_0(\int^t w_0\,\mathrm{d}t)\rangle = 0$ with the leading-order wave solution (§ 3); and the other two vanish because quadratic products of $n=0$ and $n=1$ have zero phase average since they have phase functions $\pm S$ and $\pm 2S$, respectively (§ 5). The remaining terms are $O(1)$. They can be evaluated further by substituting c_n from (10.4) and evaluating the resulting wave-averaged quantities using the leading-order wave solution (5.21) and the definition of Stokes drift (8.7), while also recognizing some cancellations due to the wave averaging. The result is

$$\frac{\partial C}{\partial T} + \left(\boldsymbol{v}\cdot\nabla_X + w^c\frac{\partial}{\partial z}\right)C = -\langle\boldsymbol{v}^{St}\rangle\cdot\nabla_X C - \langle w^{St}\rangle\frac{\partial C}{\partial z}. \tag{10.7}$$

Thus, three-dimensional tracer advection happens both by the current velocity and by the wave-averaged Lagrangian velocity composed of the horizontal Stokes drift and its associated vertical pseudo-velocity. The latter effect is a generalization of the horizontal tracer advection by $\boldsymbol{v}^{St}$ found previously (Mei & Chian 1994; Restrepo & Bona 1995; McWilliams & Restrepo 1999). The addition here of vertical advection by the pseudo-velocity w^{St} is a consequence of the horizontal spatial scale separation between waves and currents.

The leading-order long-wave tracer balance also occurs at $O(\epsilon^4)$. It thus has a right-hand-side wave-averaged forcing term analogous to (10.5)–(10.7) that selects the τ time variation instead of the T variation (n.b. (4.2), as well as long-wave advection

of the current-scale tracer gradients. The outcome is

$$\frac{\partial c^{lw}}{\partial \tau} = -(\boldsymbol{q}^{lw} + (\boldsymbol{v}^{St})^{\dagger}) \cdot \nabla_X C - (w^{lw} + (w^{St})^{\dagger}) \frac{\partial C}{\partial z} + \frac{1}{2} \frac{\partial}{\partial z} \left[\left(\frac{\partial}{\partial \tau} \overline{e^2} \right) \frac{\partial C}{\partial z} \right]. \tag{10.8}$$

The final right-hand-side term involves the variance of the vertical parcel displacement for the wave field, e, defined to leading order by

$$\frac{\partial e}{\partial t} = w \Rightarrow \overline{e^2} = \tfrac{1}{2}|e_{01}|^2, \quad e_{01} = \frac{A \sinh[\mathscr{L}]}{\sinh[\mathscr{H}]} \tag{10.9}$$

(n.b. $e = \eta$ at $z = 0$). This relation shows that long-wave tracer fluctuations are a consequence of combined long-wave velocity and Stokes-drift advection of current-scale tracer gradients, analogous to the current-scale tracer fluctuations in (10.7), plus an apparent vertical diffusion in the long-wave tracer field by temporal changes in the wave displacement variance. This final effect does not lead to an actual vertical diffusion of C in (10.7) since its $\langle \cdot \rangle$ average is zero.

11. Stratified flows

Given the preceding results, it is straightforward to generalize the formal theory to include the effects of density stratification. Here we consider the simplest case where the density itself is a material tracer, but the further extension to a more general equation of state would not be difficult. In this case all of the relations in § 10 apply to the density ρ, or equivalently the buoyancy $\mathscr{B}$ defined dimensionally by

$$\mathscr{B} = g \left(1 - \frac{\rho}{\rho_o} \right). \tag{11.1}$$

Associated with $\mathscr{B} \neq 0$ there is an additional gravitational force. If we non-dimensionalize the buoyancy by $\mathscr{B}_o = g\epsilon^3\delta$ – so that it contributes at leading order in the current vertical momentum balance in § 9.5, consistent with the criteria for the choices in (4.3) – then the non-dimensional momentum equation (2.1) generalizes to

$$\frac{\partial \boldsymbol{U}}{\partial t} + \cdots = \hat{\boldsymbol{z}} \frac{\epsilon^3 \mathscr{B}}{\tanh[\mu]}, \tag{11.2}$$

where the dots denote previous terms not repeated here. As a consequence, the vorticity equation (2.6) becomes

$$\frac{\partial \boldsymbol{\Omega}}{\partial t} + \cdots = -\hat{\boldsymbol{z}} \times \nabla \left[\frac{\epsilon^3 \mathscr{B}}{\tanh[\mu]} \right], \tag{11.3}$$

and the conserved energy (2.9) becomes

$$\mathscr{E} = \int\int_{\mathscr{D}} \int_{-\mu H}^{\epsilon E} \left(\tfrac{1}{2} \boldsymbol{U} \cdot \boldsymbol{U} + \frac{z}{\epsilon^2 \tanh[\mu]} - \frac{\epsilon^2 z' \mathscr{B}}{\tanh[\mu]} \right) \mathrm{d}z' \, \mathrm{d}\boldsymbol{x}'. \tag{11.4}$$

The effects additional to those in § 2 are, respectively, the buoyancy force, buoyancy force curl, and potential energy.

Buoyancy effects are negligible for the leading-order gravity wave solutions in § 3. Indeed they are also negligible for the wave envelope dynamics in § 5. Analogous to (4.1) and (10.2), we decompose $\mathscr{B}$ into primary- and long-wave and current components,

$$\mathscr{B} = \epsilon(b(\boldsymbol{x}, z, t, \boldsymbol{X}, \tau, T, \ldots) + \lambda b^{lw}(\boldsymbol{X}, \tau, T, \ldots)) + B(z, \boldsymbol{X}, T, \ldots). \tag{11.5}$$

With this choice the wave buoyancy force enters the momentum balance (5.2) as a right-hand-side term, $\hat{\boldsymbol{z}}\epsilon^4 b/\tanh[\mu]$. This is beyond the order of retained terms in § 5, but it does contribute to the wave vorticity balance (7.3) in § 7 as

$$\epsilon^{-2}\frac{\partial \boldsymbol{\omega}^w}{\partial t} = \cdots - \frac{\epsilon^2}{\tanh[\mu]}\,\hat{\boldsymbol{z}}\times\nabla b; \tag{11.6}$$

hence in (C 3*b*) as

$$\boldsymbol{\xi}_2^w = \cdots - \hat{\boldsymbol{z}}\times\nabla_x\left(\int^t \frac{b_0}{\tanh[\mu]}\,\mathrm{d}t\right). \tag{11.7}$$

We evaluate b_0 from the buoyancy counterpart of the first relation in (10.4):

$$b_{01} = -\frac{\partial B}{\partial z}\left(\int^t w_{01}\,\mathrm{d}t\right) = -\frac{A\sinh[\mathscr{Z}]}{\sinh[\mathscr{H}]}\,\frac{\partial B}{\partial z}. \tag{11.8}$$

Then (C 8) becomes

$$\boldsymbol{\xi}_{21}^w = \cdots - \frac{A\sinh[\mathscr{Z}]}{\tanh[\mu]\sigma\sinh[\mathscr{H}]}\,\frac{\partial B}{\partial z}\,(\hat{\boldsymbol{z}}\times\boldsymbol{k}), \tag{11.9}$$

without any analogous change in χ_{21}^w. In principle, this wave vorticity term contributes to the current vorticity and momentum balances in §§ 8–9 through the horizontal vortex force $\boldsymbol{J}$ in (8.4), specifically the term $\hat{\boldsymbol{z}}\times\langle w_0\boldsymbol{\xi}_2^w\rangle$. In practice, however, this buoyancy contribution is zero after inserting w_{01} from (5.21) and $\boldsymbol{\xi}_{21}^w$ from (11.9) and averaging. Yet the buoyancy torque in (11.3) does contribute at leading order in the current vorticity balance, providing an additional term to the horizontal equation in (8.2):

$$\frac{\partial \boldsymbol{\xi}^c}{\partial T} = \cdots - \frac{\hat{\boldsymbol{z}}}{\tanh[\mu]}\times\nabla_X B. \tag{11.10}$$

In summary, density stratification does not change the primary wave dynamics importantly. It does contribute to the current dynamics through the buoyancy force in the vertical momentum balance in (9.17),

$$\frac{\partial p^c}{\partial z} = -\frac{\partial \mathscr{K}}{\partial z} + K + \frac{B}{\tanh[\mu]}, \tag{11.11}$$

and through the buoyancy torque in (11.10). Wave-averaged advection does contribute to the evolution equation for B analogous to (10.7):

$$\frac{\partial B}{\partial T} + \left(\boldsymbol{v}\cdot\nabla_X + w^c\frac{\partial}{\partial z}\right)B = -\langle \boldsymbol{v}^{St}\rangle\cdot\nabla_X B - \langle w^{St}\rangle\frac{\partial B}{\partial z}. \tag{11.12}$$

It similarly contributes to the long-wave buoyancy equation analogous to (10.8):

$$\frac{\partial b^{lw}}{\partial \tau} = -(\boldsymbol{q}^{lw} + (\boldsymbol{v}^{St})^\dagger)\cdot\nabla_X B - (w^{lw} + (w^{St})^\dagger)\frac{\partial B}{\partial z} + \frac{1}{2}\frac{\partial}{\partial z}\left[\left(\frac{\partial}{\partial \tau}\overline{e^2}\right)\frac{\partial B}{\partial z}\right]. \tag{11.13}$$

12. Shallow-water currents and tracers

A widespread oceanic approximation for currents with small aspect ratio (i.e. $\beta \ll 1$) in a uniform-density layer is the so-called shallow-water model. In such an asymptotic limit the vertical structure of the flow is often considered to have little significance, so that it is sensible to represent the fluid velocity in terms of its depth average. This form of representation is not unique. One alternative is to represent the

velocity by its value at the ocean surface (Peregrine 1967; Restrepo & Bona 1995). Here, however, we choose the simpler alternative assumption that $\partial \boldsymbol{v}/\partial z \approx 0$. The result of this assumption is a considerably simplified dynamics compared to either the three-dimensional dynamics derived in §§ 8–10 or even their depth-averaged dynamics (Restrepo 2001). In the presence of wave-averaged forcing with non-trivial vertical structure (i.e. $\mathscr{H}$ not small), the shallow-water condition of zero vertical current shear cannot hold; however, we can imagine vertical mixing processes (absent in the present formulation) that act to enforce the shallow-water condition on the evolutionary time scale of the currents but not the waves. In such a case we can heuristically argue that this would have the effect of imposing this condition on the current and tracer dynamics.

The current vorticity (8.3) implies that $\boldsymbol{\xi}^c = 0$ to $O(\epsilon^2)$ if $\partial \boldsymbol{v}/\partial z = 0$. This greatly simplifies the wave vorticity: from (C 1)–(C 3), we conclude that $\boldsymbol{\xi}_0^w = \chi_0^w = \boldsymbol{\xi}_1^w = \chi_1^w = 0$; hence $\boldsymbol{J}$ or $\boldsymbol{J}_*$ is entirely given by its first term in (8.6) or (9.20). Ignoring the horizontal vorticity equation in (8.2) and vertically averaging the wave forcing in the vertical vorticity equation in (8.2) inside the horizontal divergence operator – both for consistency with the shallow-water condition and to preserve the differential functional form of the forcing – we obtain for the latter,

$$\frac{\partial \chi^c}{\partial T} + \nabla_X \cdot [(f + \chi^c)\boldsymbol{v}] = \hat{\boldsymbol{z}} \cdot \nabla_X \times \left[\frac{1}{\mu H} \int_{-\mu H}^{0} \boldsymbol{J} \, \mathrm{d}z \right] = -\nabla_X \cdot \left[\Pi \left\langle \int_{-\mu H}^{0} \boldsymbol{v}^{St} \, \mathrm{d}z \right\rangle \right]. \tag{12.1}$$

Here the depth-integrated Stokes drift is given by (9.13), and

$$\Pi = \frac{f + \chi^c}{\mu H} \tag{12.2}$$

is the potential vorticity of the shallow-water currents. The local mass balance from (9.14) becomes

$$\nabla_X \cdot [\mu H \boldsymbol{v}] = -\nabla_X \cdot \left\langle \int_{-\mu H}^{0} \boldsymbol{v}^{St} \, \mathrm{d}z \right\rangle. \tag{12.3}$$

These two relations can be combined to give the potential vorticity law,

$$\left(\frac{\partial}{\partial T} + \boldsymbol{v} \cdot \nabla_X \right) \Pi = -\left[\frac{1}{\mu H} \int_{-\mu H}^{0} \langle \boldsymbol{v}^{St} \rangle \, \mathrm{d}z \right] \cdot \nabla_X \Pi. \tag{12.4}$$

A further compaction of these expressions can be made by defining

$$A^z = f + \chi^c, \qquad \hat{\boldsymbol{z}} \times \nabla_X \Psi = \mu H \mathscr{U} = \mu H \boldsymbol{v} + \left\langle \int_{-\mu H}^{0} \boldsymbol{v}^{St} \, \mathrm{d}z \right\rangle, \tag{12.5}$$

that, respectively, are the vertical component of the absolute vorticity for currents A^z and the combined transport streamfunction Ψ that ensures the mass balance in (12.3). Rewriting (12.1) and (12.4), with $\Pi = A^z/\mu H$, yields

$$\left.\begin{aligned} &\frac{\partial A^z}{\partial T} + \nabla_X \cdot [A^z \mathscr{U}] = 0, \\ &\frac{\partial \Pi}{\partial T} + \mathscr{U} \cdot \nabla_X \Pi = 0. \end{aligned}\right\} \tag{12.6}$$

These are quite familiar functional forms for shallow-water vorticity and potential-vorticity dynamics, but with the Stokes advection implicit in the relevant advective velocity.

The vorticity and divergence relations (12.1)–(12.3) are sufficient to determine $\boldsymbol{v}$, given the definition of χ^c in (8.3). Thus we can avoid dealing explicitly with the current momentum balances, (9.15) and (9.17), and the associated boundary conditions, (9.3), (9.9), and (9.12); this also allows us to avoid (p^c, ζ^c, w^c) except as diagnostic fields. But the relations (9.4)–(9.8) for $\hat{p}$ and $\hat{\zeta}$ are unaltered in the shallow-water approximation.

The analogous shallow-water statement about the material tracer is $\partial C/\partial z = 0$. Both c_0 and c_1 in (10.4) vanish since they are proportional to $\partial C/\partial z$, and the leading-order tracer fluctuation occurs only at $O(\nu\epsilon^2)$ as

$$c_2 = -\nabla_X C \cdot \left(\int^t \boldsymbol{q}_0 \, \mathrm{d}t \right). \tag{12.7}$$

The corresponding slow tracer balance (10.7) becomes

$$\frac{\partial C}{\partial T} = -\boldsymbol{v} \cdot \nabla_X C - \left[\frac{1}{\mu H} \left\langle \int_{-\mu H}^{0} \boldsymbol{v}^{St} \, \mathrm{d}z \right\rangle \right] \cdot \nabla_X C \tag{12.8}$$

after the vertical averaging required for consistency with the shallow-water conditions. Thus, the wave-averaged forcing has the effect of an extra horizontal tracer advection by the depth-averaged Stokes drift.

We can combine (12.3) and (12.8) into the relation

$$\frac{\partial}{\partial T}[\mu H C] = -\nabla_X \cdot \left[\left(\mu H \boldsymbol{v} + \left\langle \int_{-\mu H}^{0} \boldsymbol{v}^{St} \, \mathrm{d}z \right\rangle \right) C \right] = -\hat{\boldsymbol{z}} \cdot \nabla_X \Psi \times \nabla_X C. \tag{12.9}$$

Integrating this over all space yields the expected conservation relation for the total material tracer,

$$\frac{\mathrm{d}}{\mathrm{d}T} \int \int_{\mathscr{D}} \int_{-\mu H}^{0} C \, \mathrm{d}z \, \mathrm{d}\boldsymbol{x} = 0, \tag{12.10}$$

if there is no flux at the lateral boundary.

13. An illustrative example: evolution of a shelf vortex

We illustrate some of the possible wave and current behaviours with numerical solutions of the shallow-water model (§ 12). We choose a broad shelf region with a gentle bottom slope up toward the west and a circular depression (figure 1*a*). We refer to the edges $x = 0$ and $y = 0$ of the rectangular domain as the western and southern boundaries. The primary wave is specified to be incident from the deeper region to the east, and it propagates westward through the domain *en route* to a coastline farther west. The currents are dominated by a cyclonic vortex, initially centred over the bottom depression (figure 1*b*). We examine both wave and current solutions, but their mutual interaction is artificially constrained to simplify this preliminary computational study: the wave field is in steady-state balance (on the τ scale) with the initial vortex, hence the long-wave component is zero, and the vortex evolution (on the T scale) is calculated with the wave field frozen in this initial state, rather than co-evolving with the currents. However, as more fully explained in § 14, the only field that is biased by this artificiality is $\Theta(\boldsymbol{X}, T)$. For oceanographic recognition, we present the quantitative results in dimensional units, although we retain our non-dimensional notation.

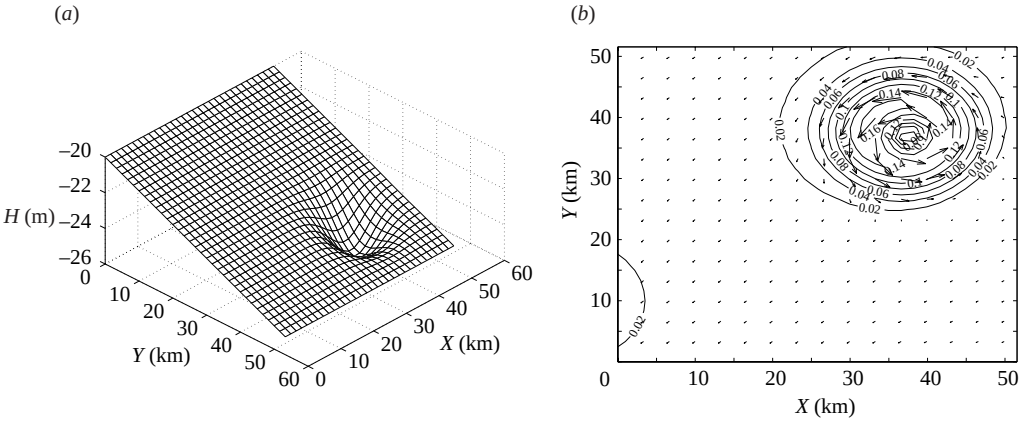

FIGURE 1. (*a*) Bottom depth $H(\boldsymbol{X})$ (m). (*b*) Initial vortex velocity $\boldsymbol{v}(\boldsymbol{X}, 0)$ (m s^{-1}).

We solve the wave equations (3.2), (5.22), and (5.35)–(5.39). In our baseline case for the wave evolution, the horizontal domain is a square with a span of $L = 56$ km. The resting depth decreases from 25 m in the east to 20 m in the west, and the superimposed depression is 2 m deep with a Gaussian decay on a spatial scale of 7 km and a centre in the northeast quadrant (figure 1*a*). The boundary conditions are periodicity in y and inward and outward radiation at the east and west, respectively. The incident wave is uniform along the eastern boundary. It has an amplitude of $|A| = 1.0$ m, slow phase of $\Theta = 0$, wavelength of $2\pi/k = 160$ m, and propagation direction to the southwest. The associated wave period is $2\pi/\sigma = 11.5$ s, phase speed is 13.6 m s^{-1}, and group velocity is $|\boldsymbol{C}_g| = 10.5$ m s^{-1}. Consequently, the non-dimensional parameters are $\epsilon = 0.04$ and $\mu = 1.0$. A cyclonic current vortex is centred over the bottom depression (figure 1*b*). It has a Gaussian shape for $\chi^c(\boldsymbol{X})$ with a peak amplitude of 10^{-4} s^{-1}. The widths of both the depression and vortex are 7 km. This is comparable to the characteristic $\boldsymbol{X}$ scale of $1/\epsilon^2 k = 15$ km to be consistent with the assumptions of the asymptotic theory (§ 4). The associated velocity field has a maximum speed of about 0.16 m s^{-1}. Note that $\boldsymbol{v}$ is not axisymmetric (n.b. stronger flow in the northwest sector than in the southeast), even though χ^c is symmetric, due to the initial velocity divergence implied by the current dynamics discussed below.

Since this partial differential equation system is hyperbolic, we use first-order space/time differencing, with upwinding in the advective terms. Nonlinear terms are incorporated using a fixed-point scheme (Isaacson & Keller 1994, pp. 109–113), iterating until the difference between successive trial solutions has an absolute supremum norm no larger than 10^{-8}. A convergence test confirms that the code has the correct approximating characteristics and that the diffusion due to first-order upwinding is small enough over the time scales of the calculations for waves propagating in any direction. The solution is integrated until reaching a steady state with the incident conditions throughout the entire domain. This takes less than 3 hr (c.f. the characteristic τ scale is $1/\sigma\epsilon^2 = 0.32$ hr).

With this posing σ is uniform in the domain because it is conserved along ray paths in (5.22); however, both $\boldsymbol{k}$ and $\boldsymbol{C}_g$ have modest variations due to the depth changes. The spatial distribution of the wave amplitude (figure 2) shows substantial variations across the domain in both magnitude and slow phase. $|A|$ is substantially reduced behind the bottom depression and increased on its flanks as a result of the convergence and divergence of $\boldsymbol{C}_g$, respectively. In the absence of the depression

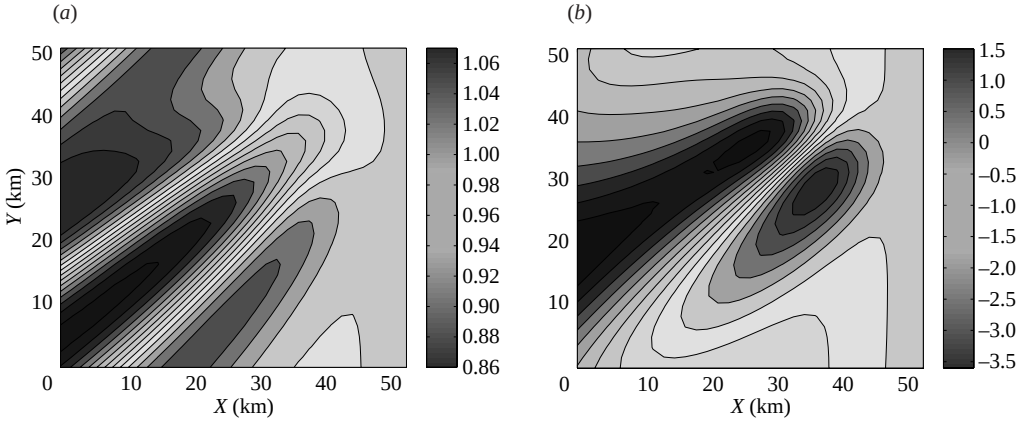

FIGURE 2. Steady-state wave amplitude in the baseline case: (*a*) $|A|(\boldsymbol{X})$ (m); (*b*) $\Theta(\boldsymbol{X})$ (rad).

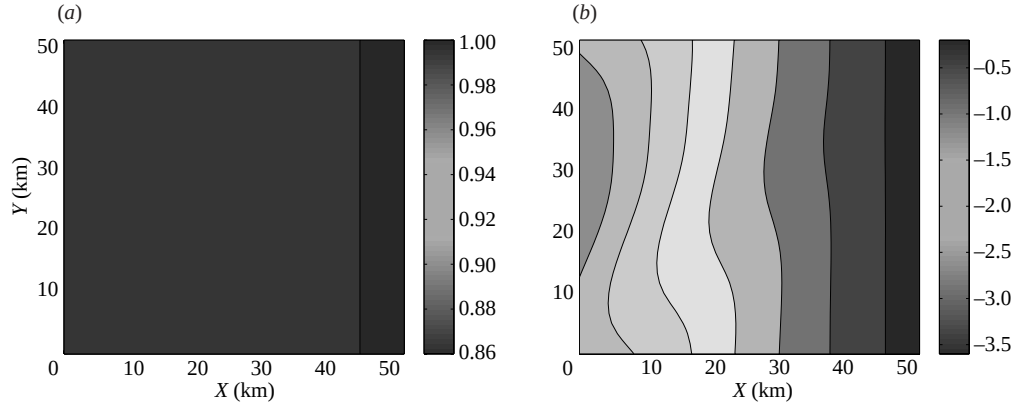

FIGURE 3. Steady-state wave amplitude: (*a*) $|A|(\boldsymbol{X})$ [m] without the bottom depression; (*b*) $\Theta(\boldsymbol{X})$ (rad) without the currents.

(figure 3*a*), $|A|$ varies much less through the small convergence of $\boldsymbol{C}_g$ as the waves shoal, and $|A|$ is uniform with uniform H. From (5.37)–(5.38), there are no influences on $|A|$ from either wave nonlinearity or currents. The Θ variations are mostly due to the wave nonlinearity (from both $\hat{\zeta}$ and M) in their magnitude (c.f. figure 3*b*), but the $\Theta(\boldsymbol{x})$ pattern in the baseline case is substantially influenced by $\boldsymbol{v}$ through opposite-sign Doppler shifting on either side of the vortex (c.f. figure 3*b*).

We solve the current equations (12.1)–(12.3). We discretize them with centred second-order differences. We make a Helmholtz decomposition,

$$\boldsymbol{v} = \hat{\boldsymbol{z}} \times \nabla_X \psi + \nabla_X \varphi, \tag{13.1}$$

and then solve the second-order elliptic equations for ψ and φ after time stepping for new values of vertical vorticity and horizontal transport divergence, respectively. The initial velocity, $\boldsymbol{v}(\boldsymbol{X}, 0)$ (figure 1*b*), thus has an axisymmetric vortical component due to χ^c and an asymmetric divergent component due to the mass-flux balance in (12.3). The boundary conditions for currents are periodicity in y (but including a trend in y for φ to represent the domain-averaged flow) and no normal flow at the eastern and

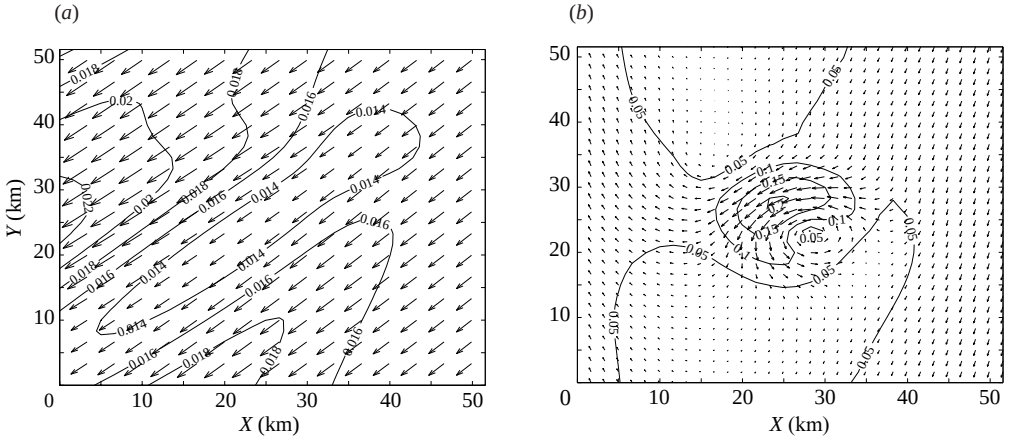

FIGURE 4. (*a*) Stokes drift $\boldsymbol{v}^{St}(\boldsymbol{X})$ (m s^{-1}) and (*b*) the combined velocity $\boldsymbol{v}+\boldsymbol{v}^{St}(\boldsymbol{X})$ (m s^{-1}) (both as vectors and contoured speeds) in the baseline case at a time of $T=4.0$ days.

western boundaries,

$$\psi=0, \qquad \frac{\partial\varphi}{\partial x}=-\frac{1}{\mu H}\left\langle \int_{-\mu H}^{0} \hat{\boldsymbol{x}}\cdot\boldsymbol{v}^{St}\,\mathrm{d}z' \right\rangle. \tag{13.2}$$

The second condition includes the Stokes drift, consistent with the mass-flux constraint (12.3). These conditions are not truly appropriate to open-ocean boundaries, but we use them only for solutions where $\boldsymbol{v}$ remains quite small there. This limits the integration time in T for solutions with spatial propagation like these. Finally we also set $\chi^c=0$ on the x boundaries for calculating the potential-vorticity flux divergence in (12.1), as a further degree of isolation of the current evolution from boundary fluxes.

In the baseline case for the current evolution, the initial cyclonic vortex (figure 1*a*) has a peak amplitude of 10^{-4} s^{-1} that is equal to f; hence the initial vortex Rossby number is 1. The depth-averaged Stokes drift, $\langle\int_{-\mu H}^{0}\boldsymbol{v}^{St}\,\mathrm{d}z'\rangle/\mu H$ is shown in figure 4(*a*). It is directed mainly to the southwest, parallel to $\boldsymbol{k}$, and its magnitude ranges from 0.013 to 0.023 m s^{-1} with a pattern similar to $|A|$ (figure 2*a*); this is slightly larger than the magnitude of $\boldsymbol{v}(0)$ (figure 1*b*). (Recall that the Stokes drift is held fixed in time.) As the currents evolve (figure 5), the vortex retains its coherence as it moves off the bottom depression and propagates to the southsouthwest at an average speed of 0.05 m s^{-1} while emitting a weak topographic Rossby wave wake. This behaviour is analogous to the much studied propagation of a strong, isolated barotropic vortex under the influence of a variable Coriolis frequency, $f(Y)$ (e.g. McWilliams & Flierl 1979), except here due to the topographic slope $H(X)$ and assisted by the Stokes-drift advection in (12.1). There is a proclivity for $\boldsymbol{v}$ to develop a component $\approx-\boldsymbol{v}^{St}$, as a means of satisfying (12.3), which would have a cancelling effect on the wave influence in the net advecting velocity. This proclivity is quite strong in wave-influenced Ekman-layer solutions (McWilliams & Restrepo 1999) but it is more modest here (c.f. Figs. 4*b* and 5*b*) where $\boldsymbol{v}^{St}$ is much weaker than $\boldsymbol{v}$.

We contrast this baseline solution with the evolution of currents without any wave influence (i.e. $\boldsymbol{v}^{St}=0$), shown in figure 6. The vortex evolution is qualitatively similar without waves, but the propagation speed and direction are substantially different, the Rossby wave wake is less extensive, and the exterior velocity field is smaller.

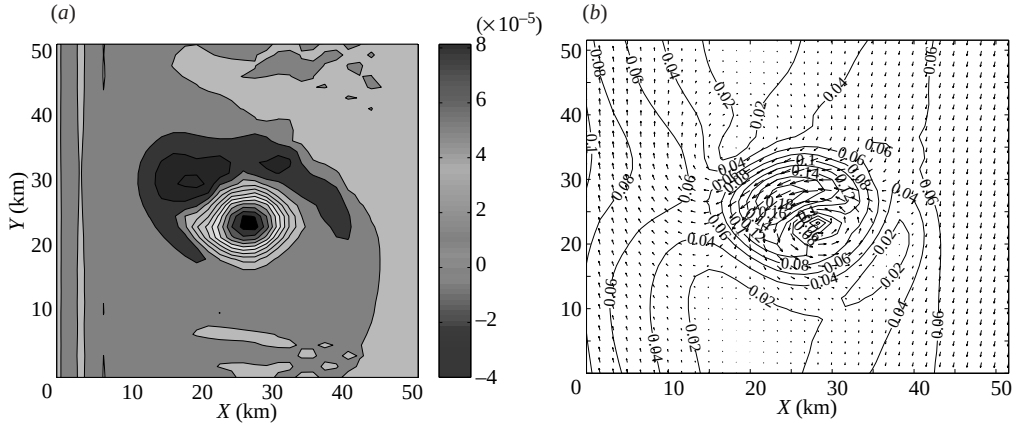

FIGURE 5. (*a*) Vorticity $\chi^c(\boldsymbol{X})$ (s^{-1}) and (*b*) velocity $\boldsymbol{v}(\boldsymbol{X})$ ($m\,s^{-1}$) (both as vector and contoured speed) for the currents in the baseline case at a time of $T = 4.0$ days.

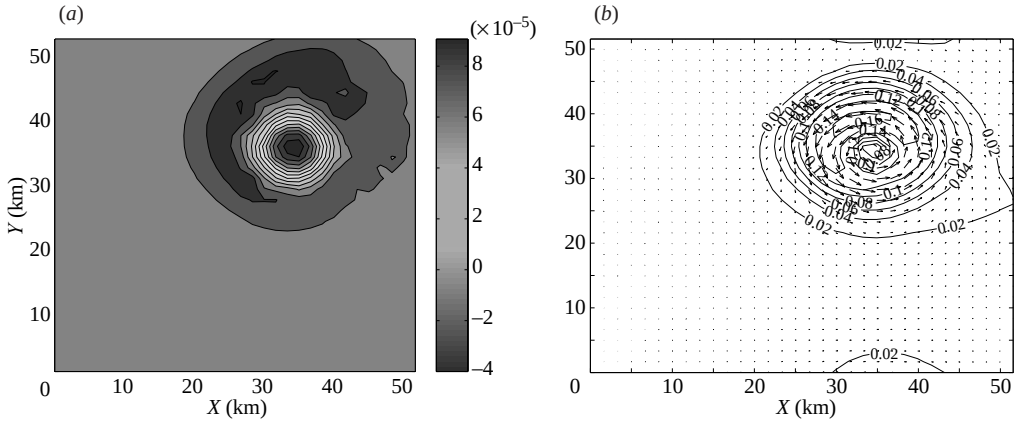

FIGURE 6. Same as figure 5, except without wave effects.

The propagation speed is here more toward westsouthwest and the average speed is $0.01\,m\,s^{-1}$. Note that the difference in propagation speeds with and without wave effects is larger than the magnitude of the Stokes drift by about a factor of 2. Since the initial vortex would be a steady solution without a topographic slope (because the bottom depression and the vortex are both axisymmetric and concentric), there is an early slowness in the propagation until the vortex moves away from the depression. The axial asymmetry in the vortex velocity, evident in the initial conditions (figure 1*b*), becomes larger with time (figure 5*b*) in the presence of the waves, but it is nearly absent without waves (figure 6). This occurs in spite of a high degree of axisymmetry persisting in χ^c in both cases.

From the differing vortex displacements with and without waves, it is clear that this solution does not conform to the misinterpretation of Ursell (1950) discussed at the end of §9.5. In particular, the net currents in the presence of the primary waves (figure 4*b*) are noticeably different from the currents without waves (figure 6*b*), both near the vortex and in the far field. The wave-averaged effects are not limited to the currents alone. It can be inferred from figure 4 that the evolution of passive tracers, advected by the net velocity in (12.9), differs significantly in the presence of primary

waves. With waves, tracer patches in the vicinity of the vortex move more rapidly to the southwest and are stirred less vigorously; nearshore patches move farther northward; and offshore patches move farther southward (for brevity these fields are not shown).

These solutions demonstrate that the effects of wave–current interactions, as implied by our asymptotic theory, can be significant in a plausible coastal regime. Here we intend no more than a preliminary impression of the implied possibilities, leaving to the future a more extensive phenomenological exploration and dynamical interpretation.

14. Summary and discussion

In this paper we have derived a leading-order asymptotic theory for the coupled evolution of a primary gravity-wave field, forced long waves, and currents. This is done in the context of a coastal shelf region with finite-depth effects on all these components. The resulting model yields a fairly complete description of the dynamics of waves, currents, buoyancy, and tracers in this setting. The principal assumptions are the following:

(*a*) The primary gravity waves have the fastest velocity scale ($\delta,\ \lambda \ll 1$); they are nearly irrotational; and they have a weakly nonlinear dynamics because of small wave slope ($\epsilon = ak \ll 1$).

(*b*) There is a scale separation in both temporal and horizontal scales between the primary wave and the currents, long waves, topography, and domain shape ($\beta,\ \gamma \ll 1$). These assumptions are embodied in the multi-scale solution form (4.1).

The asymptotic theory is first developed for a non-stratified, non-dissipative, finite-depth ocean (i.e. with a depth comparable to the primary wave scale; $\mu \sim 1$), but generalizations to deep water (§ 5.4), material tracers (§ 10), and density stratification (§ 11) are also developed. The governing equations in the theory are averaged over the primary wave scales, and thus contain horizontal and time derivatives only on longer scales. The scaling relations among the various parameters (4.3) are chosen to give the most general governing dynamical balances at leading order, consistent with the assumptions above.

The primary gravity-wave field has an oscillatory structure in time and horizontal coordinate, is surface intensified, and has the familiar linear finite-depth dispersion relation (§ 3). On the horizontal scale of the wave envelope (§ 5), the primary phase properties satisfy a topographically controlled group-velocity theory for waves in a slowly varying environment (5.22), and the amplitude function satisfies an action-conservation law (5.37)–(5.38) independent of the long waves and currents, but with slow phase modulation (5.39) by the topography, wave nonlinearity, long waves, and currents.

A long infra-gravity wave is forced by the phase-averaged Bernoulli head and horizontal mass flux of the primary wave (§ 6). It is composed of a static component involving only sea-level and pressure variations (6.3) – called wave set-up – and a dynamic component consistent with linear shallow-water waves (6.7)–(6.8). Both of these components disappear after a transient adjustment of the primary waves to their generating boundary conditions (and wind forcing, if included) when the latter are imposed in a steady-state fashion. On the other hand, a propagating primary wave packet forces propagating long waves but no currents (§ 6.5).

There are analogous static components in sea level and pressure in response to the steady-state wave-averaged Bernoulli head and horizontal mass flux (9.8). The

wave-averaged corrections to the usual hydrostatic relation between low-frequency large-scale sea level and dynamic pressure – involving both $\langle w^2 \rangle$ plus additional terms in (9.9) – need to be considered in inferences of geostrophic currents from tide-gauge and radar-altimetric measurements (c.f. McWilliams & Restrepo 1999); however, these corrections are expected to be negligible for geostrophic current inferences in deep water for small current Rossby number (n.b. the end of §§9.2 and 9.5).

The vorticity balance for the currents (8.2) contains the wave-averaged vortex force, $(\epsilon^5 \boldsymbol{J},\ \epsilon^3 K)$ or $(\epsilon^5 \boldsymbol{J}_*,\ \epsilon^3 K_*)$ in (8.6) or (9.20), related to the primary-wave horizontal Stokes drift, $\boldsymbol{v}^{St}$, and its vertical pseudo-velocity, w^{St}, by (8.7)–(8.9). Stokes drift also contributes to the depth-integrated mass balance for currents (9.14). In the current momentum balance (9.15)–(9.17), there is an additional wave-averaged Bernoulli-head force, $-\boldsymbol{\nabla}\mathscr{K}$ or $-\boldsymbol{\nabla}\mathscr{K}_*$ from (9.16) or (9.20), and a static wave set-up in sea level and pressure (9.8). Finally, due to fluctuations induced by the primary wave acting on large-scale low-frequency material-concentration gradients, there are wave-averaged advective transports in the material-tracer and buoyancy balances, (10.7) and (11.12), by $\boldsymbol{v}^{St}$ and w^{St}. The large-scale buoyancy variations, of course, couple to the current dynamics through the gravitational force in (11.10) and (11.11).

The wave–current dynamical coupling in this asymptotic theory has several causal chains that are not fully closed as feedback loops. The long-wave evolution (§6) contains primary-wave forcing that depends on the magnitude of the wave amplitude $|A|$ but not the slow phase Θ, and it also has no direct current effects; the same is true for the long-wave evolution of tracers and buoyancy (§§10–11). The current evolution is independent of the long waves and other transient adjustments of the primary waves on the τ scale. Furthermore, the wave effects on the current fields (including tracers and buoyancy) also depend only on $|A|$ but not Θ (§§8–12). The evolution of $|A|$ in (5.37), through conservation of wave action, has no influences from the currents and long waves nor from Θ, and thus it may be calculated independently. The evolution of Θ in (5.39), however, is influenced by $|A|$, long waves, and currents, but its evolution does not feed back onto any of them.

Since there are many additional effects that could be included in a more realistic wave dynamics than the asymptotic theory in §5 (e.g. Doppler shifting of the leading order for σ and wave steepening due to currents), it is important to emphasize that the derived form of the wave-averaged effects on the current dynamics should be robustly valid in their dependences on A, $\boldsymbol{k}$, etc., as long as the primary wave slope is not large, even if the evolution equations for these wave attributes are different than presented here.

The present theory for wave-averaged effects on currents encompasses its predecessors (Craik & Leibovich 1976; McWilliams & Restrepo 1999, where e.g. the vorticity forcing term is $\epsilon^3 \boldsymbol{\nabla} \times [\langle \boldsymbol{v}^{St} \rangle \times (\epsilon^2 f \hat{\boldsymbol{z}} + \boldsymbol{\omega}^c)]$, and the tracer and buoyancy forcing terms are advection only by $\langle\, \boldsymbol{v}^{St} \,\rangle$, rather than (10.7) and (11.12)). These prior forms are a subset of the more general ones here and can be derived by assuming that (*a*) the Rossby number is $O(1)$ and (*b*) the horizontal scale of the currents is comparable with that of the primary wave (e.g. as in Langmuir circulations; McWilliams *et al.* 1997). Thus, the essential basis for the new more general theory is the assumption of multiple horizontal scales (i.e. $\beta \ll 1$) applied to the currents as well as to wave-averaged quantities – with the happy side benefit that the isotropic regime for currents (i.e. $\beta = 1$ in this particular sense) is also encompassed.

The large-scale oceanic surface (Ekman) layer is modified by wave-averaged effects of several kinds, in addition to the familiar vertical Reynolds stress and material flux by boundary-layer turbulence (not considered in this paper). Most of these effects

were discussed in McWilliams & Restrepo (1999), and they can be derived from the present theory if we make the conventional large-scale assumption of a small Rossby number for both the currents and Stokes drift. In this limit, the principal Ekman-layer momentum balance contains the Stokes–Coriolis vortex force, $\boldsymbol{J}$, $\boldsymbol{J}_* \approx -f\hat{\boldsymbol{z}} \times \langle \boldsymbol{v}^{St} \rangle$ as in (8.6) or (9.20); the sea-level/surface-pressure relation contains the $\langle w_0^2(0) \rangle$ term as in (9.5); and the Stokes mass-transport divergence forcing of surface vertical velocity is as in (9.12). What is more general in the present theory, relevant even for small Rossby number, is the additional $\langle w^{St} \rangle$ vertical advection in the wave-averaged tracer and buoyancy balances in (10.7) and (11.12).

The preceding two paragraphs indicate that the conservative wave-averaged effects on currents and material tracers derived in this paper represent the most comprehensive characterization yet known. In particular, stepping outside the particular asymptotic scaling regime used here – a fruitful path for future research on wave–current interactions – the implicated wave-averaged terms can be appended to alternative fluid models to investigate the full range of wave influences from Langmuir circulations (i.e. $\beta \sim 1$, Rossby number$\rightarrow \infty$) to Ekman–Stokes currents (β, Rossby number$\rightarrow 0$). In the same spirit it may become advantageous to combine the long-wave and current dynamics in a single governing equation set with the union of the wave-averaged terms in §§6 and 8–11.

The illustrative solutions presented for the shallow-water *ansatz* (§§12–13) give only a small sample of the possible behaviours implicit in the coupled wave–current dynamics. A future task is to make a more systematic phenomenological exploration, with the plausible expectation that new modes of behaviour will be found (c.f. the Langmuir instability; Craik & Leibovich 1976). Because the asymptotic equations are averaged over the primary wave oscillations, they are much more economical to solve computationally than the primitive equations. For transient wave adjustment the reduction in computational cost is by a factor of $\beta^3 = \epsilon^6$ and, for steady-state waves (§5.4) and currents, the factor is $\beta^2\gamma = \epsilon^8$. These will allow studies of coupling regimes that are quite inaccessible by direct numerical simulation.

The present theory lacks several features needed for realistically posed problems in coastal regions. Most important are parameterizations for several non-conservative effects. These include wave and current generation by local winds, to accompany the remotely generated waves transmitted through open lateral boundaries; more robust wave boundary conditions (e.g. Higdon 1986, 1987); wave dissipation, implicitly representing the weakly nonlinear cascade from the spectrum-peak scale to breaking and viscous dissipation, as well as wave damping by surface contamination; current dissipation and boundary-layer mixing; and shoreline wave absorption and/or reflection and rip current generation through the accompanying radiation-stress divergence (Longuet-Higgins 1970). Although the present theory has been presented for a single primary wave, several such waves with incommensurate primary phase fields may be superimposed without changing the results above since $\epsilon \ll 1$; their wave-averaged effects on the long waves, currents, and material tracers are simply additive. Even if their phase fields are nearly commensurate, e.g. as might happen with shoreline reflection, then the generalization to include weakly nonlinear wave-wave coupling can be envisioned along previously developed lines (e.g. Komen *et al.* 1994, Chap. II.3).

We appreciate support from the National Science Foundation grants OCE 96-33681 (J. C. M.) and DMS 03-27642 (J. C. M. and J. M. R.) and from the National Aeronautics and Space Administration grant NAG5-11163 (J. M. R.). This work was

performed partly while J. M. R. was a summer Faculty Research Program visitor of the Mathematics and Computer Science Division at Argonne National Laboratory, as well as a visitor to the T-7 Division of Los Alamos National Laboratory.

Appendix A. Higher-order wave components

In the analyses of the current dynamics, we require a full determination of the wave quantities at $O(\epsilon)$ for $m=2$ and $O(\epsilon^2)$ for $m=1$. Here we make these determinations for all quantities except the wave vorticity (§ 7 and Appendix C) using expansion forms like those in (5.24).

The velocity potential has components ϕ_{01} and ϕ_{12} given by (5.18) and (5.31). The boundary-value problem for ϕ_{21} is posed in (5.27) with forcing terms in (5.33), under the compatibility constraint provided by the amplitude equation (5.35). The latter can be expressed as

$$\begin{aligned}\tilde{F}_{21}\int_{-\mu H}^{0}\cosh^2[\mathscr{Z}']\frac{\partial^2\mathscr{V}}{\partial z'^2}\,\mathrm{d}z' &+ \frac{F_{21}^{c}}{4k\cosh[\mathscr{H}]}(2\mathscr{H}+\sinh[2\mathscr{H}])\\ &+\frac{F_{21}^{s}}{4k\cosh[\mathscr{H}]}(\cosh[2\mathscr{H}]-1)+\frac{F_{21}^{\mathscr{Z}s}}{8k\cosh[\mathscr{H}]}(2\mathscr{H}\cosh[2\mathscr{H}]-\sinh[2\mathscr{H}])\\ &= \tanh[\mu]G_{21}-\frac{B_{21}}{\cosh[\mathscr{H}]},\end{aligned}\tag{A 1}$$

where we have partitioned F_{21} in (5.33) into its separate dependences on $\mathscr{Z}$:

$$\left.\begin{aligned}F_{21}^{c} &= -\frac{1}{\tanh[\mu]}\left(2\boldsymbol{k}\cdot\nabla_X\left[\frac{A}{\sigma\cosh[\mathscr{H}]}\right]+\frac{A}{\sigma\cosh[\mathscr{H}]}(\nabla_X\cdot\boldsymbol{k})\right),\\ F_{21}^{s} &= -\frac{2Ak}{\tanh[\mu]\sigma\cosh[\mathscr{H}]}(\boldsymbol{k}\cdot\nabla_X)\mu H,\\ F_{21}^{\mathscr{Z}s} &= -\frac{2A}{\tanh[\mu]\sigma k\cosh[\mathscr{H}]}(\boldsymbol{k}\cdot\nabla_X)k,\\ \tilde{F}_{21} &= -\frac{i2A}{k\tanh[\mu]\sinh[2\mathscr{H}]}.\end{aligned}\right\}\tag{A 2}$$

The solution to the boundary-value problem is

$$\begin{aligned}\phi_{21} = &-\frac{\mathrm{i}A}{2k^2\sinh[\mathscr{H}]}\left(\frac{\partial\mathscr{V}}{\partial z}(z)+\frac{\partial\mathscr{V}}{\partial z}(-\mu H)\right)\sinh[\mathscr{Z}]-\frac{A\sigma(\boldsymbol{k}\cdot\nabla_X[\mu H])}{k^2\sinh[\mathscr{H}]}\mathscr{Z}\cosh[\mathscr{Z}]\\ &+\frac{\mathrm{i}A}{2k^2\sinh[\mathscr{H}]}\left(\int_{-\mu H}^{z}\frac{\partial^2\mathscr{V}}{\partial z'^2}\sinh[2\mathscr{Z}'-\mathscr{Z}]\,\mathrm{d}z'\right)\\ &-\frac{\sigma\cosh[\mathscr{H}]}{kA}\nabla_X\cdot\left[\frac{A^2\boldsymbol{k}}{k^2\sinh[2\mathscr{H}]}\right]\mathscr{Z}\sinh[\mathscr{Z}]-\frac{A\sigma(\boldsymbol{k}\cdot\nabla_X)k}{2k^4\sinh[\mathscr{H}]}\mathscr{Z}^2\cosh[\mathscr{Z}].\end{aligned}\tag{A 3}$$

We have set to zero the undetermined coefficient of the homogeneous solution, $\cosh[\mathscr{Z}]$, to distinguish it from the leading-order solution in (5.18).

From (5.15) expressed in the form of (5.28), we derive the sea-level component at this order,

$$\eta_{21} = \mathrm{i}\tanh[\mu]\sigma\phi_{21}(0)+H_{21},\tag{A 4}$$

where

$$H_{21} = \mathrm{i}\frac{\partial}{\partial\tau}\left[\frac{A}{\sigma}\right] + Ak\tanh[\mathscr{H}]\,Z - \frac{A}{\sigma}\,\mathscr{V}(0) - \frac{3|A|^2Ak^2}{8}\left(\frac{\sinh^4[\mathscr{H}]-\sinh^2[\mathscr{H}]+1}{\sinh^4[\mathscr{H}]}\right). \tag{A 5}$$

The wave velocity at higher order comes from evaluating (5.1) in terms of ϕ and $\boldsymbol{v}$, using (5.32) for $\boldsymbol{u}^{wv}$:

$$\left.\begin{aligned} \boldsymbol{q}_{12} &= 2\mathrm{i}\boldsymbol{k}\phi_{12} = \frac{3A^2\sigma\boldsymbol{k}}{4\sinh^4[\mathscr{H}]}\,\cosh[2\mathscr{Z}],\\ w_{12} &= \phi_{12,z} = -\frac{3\mathrm{i}A^2\sigma k}{4\sinh^4[\mathscr{H}]}\,\sinh[2\mathscr{Z}],\\ \boldsymbol{q}_{21} &= \mathrm{i}\boldsymbol{k}\phi_{21} - \mathrm{i}\nabla_X\left[\frac{A\sigma\cosh[\mathscr{Z}]}{k\sinh[\mathscr{H}]}\right] - \frac{A\sinh[\mathscr{Z}]}{\sinh[\mathscr{H}]}\frac{\partial\boldsymbol{V}}{\partial z},\\ w_{21} &= \frac{\partial}{\partial z}\phi_{21} + \frac{\mathrm{i}A\cosh[\mathscr{Z}]}{k\sinh[\mathscr{H}]}\frac{\partial\mathscr{V}}{\partial z}. \end{aligned}\right\} \tag{A 6}$$

These expressions have been checked by verifying the incompressibility relation in (2.1) for each (n, m) component. Finally, the wave pressure components are derived from the Bernoulli relation (5.4),

$$\left.\begin{aligned} p_{12}^w &= 2\mathrm{i}\sigma\phi_{12} - \frac{A^2k}{2\tanh[\mu]\sinh[2\mathscr{H}]} = \frac{A^2k}{2\tanh[\mu]\sinh[2\mathscr{H}]}\left(3\frac{\cosh[2\mathscr{Z}]}{\sinh^2[\mathscr{H}]}-1\right),\\ p_{21}^w &= \mathrm{i}\sigma\phi_{21} + \mathrm{i}\frac{\partial}{\partial\tau}\left[\frac{A\sigma\cosh[\mathscr{Z}]}{k\sinh[\mathscr{H}]}\right] - \frac{A\sigma\cosh[\mathscr{Z}]}{k\sinh[\mathscr{H}]}\,\mathscr{V} - \frac{3|A|^2Ak^2}{4\tanh[\mu]}\frac{\cosh[3\mathscr{Z}]}{\sinh[2\mathscr{H}]\sinh^3[\mathscr{H}]}. \end{aligned}\right\} \tag{A 7}$$

Again, the long-wave and current effects appear in (A 3)–(A 7) only in combination as their sum.

Appendix B. Wave-averaged forcing of infra-gravity waves

The right-hand side of the momentum equation in (2.1), after substituting the primary wave solution form from (4.1) and (5.16) and isolating the phase-averaged fluctuation, has a contribution at $O(\epsilon^3)$ that is the horizontal component of

$$-\left(\left(\nabla\times\boldsymbol{u}_0^{wv}\right)\times\boldsymbol{u}_0\right)^{\dagger}.$$

By substituting for $\boldsymbol{u}_0$ from (5.21) and for $\boldsymbol{u}_0^{wv}$ from (5.32), and using the property of the phase-averaging operator that

$$\overline{ab} = 0$$

for any wave quantities a and b unless they have the same $\exp(\mathrm{i}mS/\epsilon^2)$ harmonic factor and their coefficients of A are either both real or both imaginary, this contribution can be shown to vanish. The right-hand side of the surface kinematic condition in (2.3) at $O(\epsilon^3)$, after expansion about $z = 0$ and isolation of the phase-averaged fluctuation,

becomes

$$
\begin{aligned}
&-\frac{1}{\epsilon^2}\left(\eta\frac{\partial w}{\partial z}(0)\right)^\dagger-\frac{1}{2\epsilon}\left(\eta^2\frac{\partial^2 w}{\partial z^2}(0)\right)^\dagger-\zeta\left(\eta\frac{\partial^2 w}{\partial z^2}(0)\right)^\dagger-\frac{1}{6}\left(\eta^3\frac{\partial^3 w}{\partial z^3}(0)\right)^\dagger\\
&\quad+\frac{1}{\epsilon^2}\left((\boldsymbol{q}(0)\cdot\nabla_x)\eta\right)^\dagger+\frac{1}{\epsilon}\left(\eta\left(\frac{\partial \boldsymbol{q}}{\partial z}(0)\cdot\nabla_x\right)\eta\right)^\dagger+\zeta\left(\left(\frac{\partial \boldsymbol{q}}{\partial z}(0)\cdot\nabla_x\right)\eta\right)^\dagger\\
&\quad-\left(\eta^{lw}\left(\overline{\eta\frac{\partial^2 w}{\partial z^2}(0)-\left(\frac{\partial \boldsymbol{q}}{\partial z}(0)\cdot\nabla_x\right)\eta}\right)\right)^\dagger+\frac{1}{2}\left(\eta^2\left(\frac{\partial^2 \boldsymbol{q}}{\partial z^2}(0)\cdot\nabla_x\right)\eta\right)^\dagger\\
&=\nabla_X\cdot\left(\eta_0\boldsymbol{q}_0(0)\right)^\dagger+\left(\eta_0\nabla_x\cdot\left(\frac{\partial \boldsymbol{q}_0}{\partial z}\eta_1+\frac{\partial \boldsymbol{q}_1}{\partial z}\eta_0\right)+\eta_1\nabla_x\cdot\left(\frac{\partial \boldsymbol{q}_0}{\partial z}\eta_0\right)\right)^\dagger\\
&\quad+\frac{1}{2}\left(\eta_0^2\nabla_x\cdot\left(\frac{\partial^2 \boldsymbol{q}_0}{\partial z^2}\eta_0\right)\right)^\dagger\\
&=\nabla_X\cdot\left(\eta_0\boldsymbol{q}_0(0)\right)^\dagger. \qquad \text{(B 1)}
\end{aligned}
$$

In deriving the successive relations in (B 1), we use the following: the incompressibility condition for the wave field; the ϵ expansion (5.16) and wave solution form (5.24); the result above for what is required to have a non-zero phase-average – which is true here only for the term in the final relation in (B 1) since both $\boldsymbol{q}_n$ and η_n have purely real coefficients for $n = 0, 1$, see (5.18), (5.21), (5.31), and (A 6); the related property that

$$\overline{\nabla_x\cdot a\boldsymbol{b}}=\epsilon^2\nabla_X\cdot\overline{a\boldsymbol{b}}$$

for any wave quantities a and $\boldsymbol{b}$; and, finally, the property that $(\eta_0\nabla_x\cdot(\boldsymbol{q}_{0z}\eta_0))^\dagger=0$ since no triple product of $m = 1$ harmonic functions can have a non-zero average. These evaluations confirm the results in (6.1).

Appendix C. Wave vorticity solutions

After substituting (7.1) into (7.3), separating horizontal and vertical components, expanding the wave fields in ϵ, and formally integrating in time while neglecting any slow time dependences, we obtain the following relations:

$$\boldsymbol{\xi}_0^w=(\boldsymbol{\xi}^c\cdot\nabla_x)\left(\int^t\boldsymbol{q}_0\,\mathrm{d}t\right)-\frac{\partial\boldsymbol{\xi}^c}{\partial z}\left(\int^t w_0\,\mathrm{d}t\right), \qquad \text{(C 1}a\text{)}$$

$$\chi_0^w=(\boldsymbol{\xi}^c\cdot\nabla_x)\left(\int^t w_0\,\mathrm{d}t\right), \qquad \text{(C 1}b\text{)}$$

$$
\begin{aligned}
\boldsymbol{\xi}_1^w&=(\boldsymbol{\xi}^c\cdot\nabla_x)\left(\int^t\boldsymbol{q}_1\,\mathrm{d}t\right)-\frac{\partial\boldsymbol{\xi}^c}{\partial z}\left(\int^t w_1\,\mathrm{d}t\right)\\
&\quad+\int^t\left((\boldsymbol{\xi}_0^w\cdot\nabla_x)\boldsymbol{q}_0+\chi_0^w\frac{\partial\boldsymbol{q}_0}{\partial z}-(\boldsymbol{q}_0\cdot\nabla_x)\boldsymbol{\xi}_0^w-w_0\frac{\partial\boldsymbol{\xi}_0^w}{\partial z}\right)'\mathrm{d}t \qquad \text{(C 2}a\text{)}
\end{aligned}
$$

$$
\begin{aligned}
\chi_1^w&=(\boldsymbol{\xi}^c\cdot\nabla_x)\left(\int^t w_1\,\mathrm{d}t\right)\\
&\quad+\int^t\left((\boldsymbol{\xi}_0^w\cdot\nabla_x)w_0+\chi_0^w\frac{\partial w_0}{\partial z}-(\boldsymbol{q}_0\cdot\nabla_x)\chi_0^w-w_0\frac{\partial\chi_0^w}{\partial z}\right)'\mathrm{d}t, \qquad \text{(C 2}b\text{)}
\end{aligned}
$$

$$\begin{aligned}\boldsymbol{\xi}_2^w = \hat{\boldsymbol{\xi}}_2^w + \hat{\hat{\boldsymbol{\xi}}}_2^w &+ (\chi^c + f)\left(\int^t \frac{\partial \boldsymbol{q}_0}{\partial z}\,\mathrm{d}t\right) - \left(\left(\int^t \boldsymbol{q}_0\,\mathrm{d}t\right)\cdot\nabla_X\right)\boldsymbol{\xi}^c \\ &- (\boldsymbol{V}\cdot\nabla_x)\left(\int^t \boldsymbol{\xi}_0^w\,\mathrm{d}t\right) + (\boldsymbol{\xi}^c\cdot\nabla_x)\left(\int^t \boldsymbol{q}_2\,\mathrm{d}t\right) - \frac{\partial \boldsymbol{\xi}^c}{\partial z}\left(\int^t w_2\,\mathrm{d}t\right) + \left(\int^t \chi_0^w\,\mathrm{d}t\right)\frac{\partial \boldsymbol{v}}{\partial z} \\ &+ \int^t \left((\boldsymbol{\xi}_0^w\cdot\nabla_x)\boldsymbol{q}_1 + (\boldsymbol{\xi}_1^w\cdot\nabla_x)\boldsymbol{q}_0 + \chi_0^w\frac{\partial \boldsymbol{q}_1}{\partial z} + \chi_1^w\frac{\partial \boldsymbol{q}_0}{\partial z}\right)'\,\mathrm{d}t \\ &- \int^t \left((\boldsymbol{q}_0\cdot\nabla_x)\boldsymbol{\xi}_1^w + (\boldsymbol{q}_1\cdot\nabla_x)\boldsymbol{\xi}_0^w + w_0\frac{\partial \boldsymbol{\xi}_1^w}{\partial z} + w_1\frac{\partial \boldsymbol{\xi}_0^w}{\partial z}\right)'\,\mathrm{d}t + \cdots, \end{aligned} \tag{C 3a}$$

$$\begin{aligned}\chi_2^w = \hat{\chi}_2^w + \hat{\hat{\chi}}_2^w &+ (\chi^c + f)\left(\int^t \frac{\partial w_0}{\partial z}\,\mathrm{d}t\right) - \left(\int^t w_0\,\mathrm{d}t\right)\frac{\partial \chi^c}{\partial z} \\ &+ (\boldsymbol{\xi}^c\cdot\nabla_x)\left(\int^t w_2\,\mathrm{d}t\right) - (\boldsymbol{V}\cdot\nabla_x)\left(\int^t \chi_0^w\,\mathrm{d}t\right) \\ &+ \int^t \left((\boldsymbol{\xi}_0^w\cdot\nabla_x)w_1 + (\boldsymbol{\xi}_1^w\cdot\nabla_x)w_0 + \chi_0^w\frac{\partial w_1}{\partial z} + \chi_1^w\frac{\partial w_0}{\partial z}\right)'\,\mathrm{d}t \\ &- \int^t \left((\boldsymbol{q}_0\cdot\nabla_x)\chi_1^w + (\boldsymbol{q}_1\cdot\nabla_x)\chi_0^w + w_0\frac{\partial \chi_1^w}{\partial z} + w_1\frac{\partial \chi_0^w}{\partial z}\right)'\,\mathrm{d}t + \cdots. \end{aligned} \tag{C 3b}$$

The contributions $(\hat{\boldsymbol{\xi}}_2^w, \hat{\chi}_2^w)$ are due to $(\boldsymbol{X}, \tau)$ derivatives of the $(n, m) = (0, 1)$ coefficients:

$$\left.\begin{aligned}\hat{\boldsymbol{\xi}}_{21}^w &= \frac{\mathrm{i}}{\sigma}\left((\boldsymbol{\xi}^c\cdot\nabla_X)\boldsymbol{q}_{01} - \frac{\partial}{\partial\tau}\boldsymbol{\xi}_{01}^w\right), \\ \hat{\chi}_{21}^w &= \frac{\mathrm{i}}{\sigma}\left((\boldsymbol{\xi}^c\cdot\nabla_X)w_{01} - \frac{\partial}{\partial\tau}\chi_{01}^w\right).\end{aligned}\right\} \tag{C 4}$$

The contributions $(\hat{\hat{\boldsymbol{\xi}}}_2^w, \hat{\hat{\chi}}_2^w)$ are due to the long-wave vorticity, and they have a form analogous to (C 1):

$$\left.\begin{aligned}\hat{\hat{\boldsymbol{\xi}}}_2^w &= \epsilon^{-2}\left((\boldsymbol{\xi}^{lw}\cdot\nabla_x)\left(\int^t \boldsymbol{q}_0\,\mathrm{d}t\right) - \frac{\partial \boldsymbol{\xi}^{lw}}{\partial z}\left(\int^t w_0\,\mathrm{d}t\right)\right), \\ \hat{\hat{\chi}}_2^w &= \epsilon^{-2}\left((\boldsymbol{\xi}^{lw}\cdot\nabla_x)\left(\int^t w_0\,\mathrm{d}t\right)\right).\end{aligned}\right\} \tag{C 5}$$

The right-hand-side quantities are $O(1)$ by (6.12).

The wave-vorticity expressions at $n = 0$ are equivalent to those that come from taking the curl and time integral of the wave-momentum balance (5.5) at its leading order. The neglected terms at $n = 2$ in (C 3), denoted by $\ldots$, indicate contributions from nonlinear products that yield other harmonics in the wave vorticity than $m = 1$, which at this order do not contribute to the wave-averaged fluxes in § 8. Note that we have not expanded the current quantities in ϵ since our purpose here is to obtain expressions for the functional dependence of the waves on the currents for later substitution into wave-averaged forcing terms in the current dynamical balances (§§ 8–10).

The expression (C 1) is easily evaluated to give the leading-order wave-vorticity coefficients,

$$\left.\begin{aligned}\boldsymbol{\xi}_{01}^w &= -\frac{A}{k\sinh[\mathscr{H}]}\left(\cosh[\mathscr{Z}]\mathscr{X}\,\boldsymbol{k} + k\sinh[\mathscr{Z}]\,\frac{\partial \boldsymbol{\xi}^c}{\partial z}\right), \\ \chi_{01}^w &= \frac{\mathrm{i}A}{\sinh[\mathscr{H}]}\sinh[\mathscr{Z}]\mathscr{X},\end{aligned}\right\} \tag{C 6}$$

where

$$\mathscr{X} = \boldsymbol{k}\cdot\left(\hat{\boldsymbol{z}}\times\frac{\partial \boldsymbol{v}}{\partial z}\right) \approx \boldsymbol{k}\cdot\boldsymbol{\xi}^c.$$

The coefficients (C 6) can also be obtained as the curl of $\boldsymbol{u}_0^{wv}$ in (5.32) or, equivalently, the curl of $\boldsymbol{u}_2$ in (A 6).

The expression (C 2) may similarly be evaluated to give

$$\left.\begin{aligned}\boldsymbol{\xi}_{12}^w &= -\frac{A^2}{4\sinh^2[\mathscr{H}]}\left(\frac{3\cosh[2\mathscr{Z}]}{\sinh^2[\mathscr{H}]}\mathscr{X}\boldsymbol{k} + \frac{3k\sinh[2\mathscr{Z}]}{2\sinh^2[\mathscr{H}]}\frac{\partial\boldsymbol{\xi}^c}{\partial z},\right.\\ &\qquad \left. -\frac{\sinh[2\mathscr{Z}]}{k}\frac{\partial\mathscr{X}}{\partial z}\boldsymbol{k} - \sinh^2[\mathscr{Z}]\frac{\partial^2\boldsymbol{\xi}^c}{\partial z^2}\right)\\ \chi_{12}^w &= -\frac{\mathrm{i}A^2}{2\sinh^2[\mathscr{H}]}\left(\sinh^2[\mathscr{Z}]\frac{\partial\mathscr{X}}{\partial z} - \frac{3k\sinh[2\mathscr{Z}]}{2\sinh^2[\mathscr{H}]}\mathscr{X}\right).\end{aligned}\right\} \tag{C 7}$$

Finally, the evaluation of (C 3)–(C 4) yields

$$\begin{aligned}\boldsymbol{\xi}_{21}^w = &-\frac{1}{\sigma}\left(\mathscr{X}\boldsymbol{q}_{21} + \mathrm{i}w_{21}\frac{\partial\boldsymbol{\xi}^c}{\partial z}\right) + \frac{\mathrm{i}A}{k\sinh[\mathscr{H}]}\left(k\sinh[\mathscr{Z}](\chi^c + f)\boldsymbol{k}\right.\\ &\left. - \cosh[\mathscr{Z}](\boldsymbol{k}\cdot\nabla_X)\boldsymbol{\xi}^c + \frac{\mathrm{i}}{\sigma}\left(k\sinh[\mathscr{Z}]\left(\mathscr{X}\frac{\partial\boldsymbol{v}}{\partial z} + \mathscr{V}\frac{\partial\boldsymbol{\xi}^c}{\partial z}\right) + \cosh[\mathscr{Z}]\mathscr{X}\mathscr{V}\boldsymbol{k}\right)\right)\\ &+ \frac{\mathrm{i}}{\sigma}(\boldsymbol{\xi}^c\cdot\nabla_X)\left[\frac{A\sigma\cosh[\mathscr{Z}]}{k\sinh[\mathscr{H}]}\boldsymbol{k}\right] + \frac{\mathrm{i}}{\sigma}\frac{\partial}{\partial\tau}\left[\frac{A\mathscr{X}\cosh[\mathscr{Z}]}{k\sinh[\mathscr{H}]}\boldsymbol{k}\right] + \frac{\mathrm{i}}{\sigma}\frac{\partial\boldsymbol{\xi}^c}{\partial z}\frac{\partial}{\partial\tau}\left[\frac{A\sinh[\mathscr{Z}]}{\sinh[\mathscr{H}]}\right]\\ &+ \frac{A^*}{2k\sinh[\mathscr{H}]}\left(\cosh[\mathscr{Z}]\left(\left(\boldsymbol{k}\cdot\boldsymbol{\xi}_{12}^w\right)\boldsymbol{k} + 2k^2\boldsymbol{\xi}_{12}^w\right) + k\sinh[\mathscr{Z}]\left(\frac{\partial\boldsymbol{\xi}_{12}^w}{\partial z} + \mathrm{i}\chi_{12}^w\boldsymbol{k}\right)\right)\\ &+ \frac{3|A|^2A}{8\sinh^5[\mathscr{H}]}\left(3k\cosh[3\mathscr{Z}]\mathscr{X}\boldsymbol{k} + (\sinh[3\mathscr{Z}] + \cosh[2\mathscr{Z}]\sinh[\mathscr{Z}])\frac{\partial\mathscr{X}}{\partial z}\boldsymbol{k}\right.\\ &\left. + k^2\sinh[3\mathscr{Z}]\frac{\partial\boldsymbol{\xi}^c}{\partial z} + k\sinh[2\mathscr{Z}]\sinh[\mathscr{Z}]\frac{\partial^2\boldsymbol{\xi}^c}{\partial z^2}\right) + \hat{\hat{\boldsymbol{\xi}}}_{21}^w,\end{aligned} \tag{C 8a}$$

$$\begin{aligned}\chi_{21}^w = &-\frac{1}{\sigma}\mathscr{X}w_{21} + \frac{A}{\sinh[\mathscr{H}]}\left(k\cosh[\mathscr{Z}](\chi^c + f) - \sinh[\mathscr{Z}]\frac{\partial\chi^c}{\partial z} + \mathrm{i}\frac{\sinh[\mathscr{Z}]}{\sigma}\mathscr{V}\mathscr{X}\right)\\ &+ \frac{1}{\sigma}(\boldsymbol{\xi}^c\cdot\nabla_X)\left[\frac{A\sigma\sinh[\mathscr{Z}]}{\sinh[\mathscr{H}]}\right] + \frac{1}{\sigma}\frac{\partial}{\partial\tau}\left[\frac{A\mathscr{X}\sinh[\mathscr{Z}]}{\sinh[\mathscr{H}]}\right]\\ &+ \frac{A^*}{2\sinh[\mathscr{H}]}\left(k\cosh[\mathscr{Z}]\chi_{12}^w - \mathrm{i}\sinh[\mathscr{Z}]\left(\boldsymbol{k}\cdot\boldsymbol{\xi}_{12}^w\right)\right)\\ &- \mathrm{i}\frac{3|A|^2Ak}{8\sinh^5[\mathscr{H}]}\left(k\sinh[3\mathscr{Z}]\mathscr{X} + \sinh[2\mathscr{Z}]\sinh[\mathscr{Z}]\frac{\partial\mathscr{X}}{\partial z}\right) + \hat{\hat{\chi}}_{21}^w.\end{aligned} \tag{C 8b}$$

The double-hatted terms are from (C 5). More generally we see that the long-wave and current velocities enter into the wave-vorticity expressions (C 6)–(C 8) in such a way that every term has at least one vertical derivative, and the only places where long-wave contributions appear in $(\boldsymbol{\xi}_n^w, \chi_n^w)$ are in the two terms at $n = 2$ proportional to $\mathscr{V}$, as well as the double-hatted terms. In neither case do these potential long-wave contributions survive in the wave-averaged forcing of the current vorticity equation (§ 8). The expressions (C 6)–(C 8) have been checked by verifying the non-divergence of wave vorticity for each (n, m) component.

Appendix D. Definitions of symbols

As this paper is of atypical mathematical complexity, a list of symbols is provided in table 1.

Symbol	Name	Where defined
a, A	wave sea level amplitude	(3.1), (5.18)
A^z	absolute vertical vorticity for currents	(12.5)
$\mathscr{A}$	wave action density	(5.38)
b	wave buoyancy field	(11.5)
B	current buoyancy field	(11.5)
B_{nm}	bottom wave forcing	(5.26)
$\mathscr{B}$	total buoyancy field	(11.1)
$\mathscr{B}_o$	dimensional scale for $\mathscr{B}$	after (11.1)
c	wave material concentration	(10.2)
C	current material concentration	(10.2)
C_b	Bernoulli constant	(5.4)
C_p	pressure constant	(9.4)
$\mathscr{C}$	total material concentration	before (2.1)
$\boldsymbol{C}_g$	group velocity	(5.23)
C^{lw}	long gravity-wave speed	(6.9)
$\mathscr{D}$	domain area	before (2.1)
$\delta\mathscr{D}$	domain lateral boundary	before (2.1)
e	wave vertical parcel displacement	(10.9)
E	total sea level anomaly	before (2.1)
$\mathscr{E}$	total energy	(2.9), (11.4)
$\overline{\mathscr{E}}$	mean wave energy	(3.5)
f, f_0, f^{nd}	Coriolis frequency	(2.1), (4.3)
F_{nm}	surface wave forcing	(5.25)
F_{21}^c, F_{21}^s, $F_{21}^{\mathscr{D}s}$, $\tilde{F}_{21}$	coefficients in F_{21}	(A 2)
$\tilde{\mathscr{F}}^{lw}$	dynamical forcing of long waves	(6.10)
g	gravitational acceleration	before (2.1)
G_{nm}	interior wave forcing	(5.28)
H	resting bottom depth	before (2.1)
H_{nm}	surface wave forcing of η	(5.27)
$\mathscr{H}$	rescaled depth	after (3.1)
$\boldsymbol{J}$, $\boldsymbol{J}_*$	horizontal vortex force at $O(\epsilon^5)$	(8.4), (9.20)
$\boldsymbol{k}$	horizontal wavenumber vector	(3.1)
k	modulus of $\boldsymbol{k}$	before (2.1)
K, K_*	vertical vortex force at $O(\epsilon^3)$	(8.5), (9.20)
$\mathscr{K}$, $\mathscr{K}_*$	Bernoulli head at $O(\epsilon^3)$	(9.16), (9.20)
L	computational domain width	Sec. 13
M	nonlinear coefficient in A eqn.	(5.34)
$\mathscr{M}$	total mass	(2.8)
p^w	wave pressure	(4.1)
p^{lw}	long-wave pressure	(4.1)
$\hat{p}^{lw}$,$\tilde{p}^{lw}$	components of p^{lw}	(6.3) *et seq.*
p^c, $\hat{p}$	components of current pressure	(9.1)
P, p	pressure	(2.1), (2.4)
P_0	atmospheric pressure	(2.3)
$\mathscr{P}_0$	wave-averaged pressure forcing	(9.10)
$\boldsymbol{q}$	wave horizontal velocity	(4.1)
$\boldsymbol{q}^{lw}$	long-wave horizontal velocity	(4.1)
$\boldsymbol{q}^{wv}$	vortical wave horizontal velocity	(5.32)
$\boldsymbol{Q}$	total horizontal velocity	before (2.1)
r	current pressure	(4.1)

TABLE 1. List of symbols.

Symbol	Name	Where defined
$\mathscr{R}[\cdot]$	Taylor series operator	(5.12)
S	wave phase function	(5.17), (5.19)
t	wave time coordinate	before (2.1)
T	current time coordinate	(4.1)
$\boldsymbol{T}^{St}$	depth-integrated Stokes velocity	(6.2) & (9.13)
$\boldsymbol{U}$	total 3D velocity	before (2.1)
$\boldsymbol{u}$	total 3D wave velocity	(4.1)
$\boldsymbol{u}^{lw}$	3D long-wave velocity	(4.1)
$\boldsymbol{u}^{wv}$	vortical part of 3D wave velocity	(5.1)
$\mathscr{U}$	combined current and Stokes-drift horizontal transport velocity	(12.5)
$\boldsymbol{v}$	horizontal current velocity	(4.1)
$\boldsymbol{v}^{St}$	Stokes-drift velocity	(8.7)
$\boldsymbol{V}$	phase-averaged horizontal velocity	(5.3)
$\mathscr{V}$	wavevector-$\boldsymbol{V}$ dot product	after (5.33)
w	wave vertical velocity	(4.1)
w^c	current vertical velocity	(4.1)
w^{lw}	long-wave vertical velocity	(4.1)
w^{wv}	vortical wave vertical velocity	(5.32)
w^{St}	Stokes-drift vertical pseudo-velocity	(8.9)
W	total vertical velocity	before (2.1)
$\boldsymbol{x} = (x, y)$	wave-scale horizontal coordinates	before (2.1)
$\boldsymbol{X}$	slow horizontal coordinates	before (4.1)
$\mathscr{X}$	wavenumber-vorticity product	after (C 6)
z	vertical coordinate	before (2.1)
$\hat{\boldsymbol{z}}$	upward vertical unit vector	before (2.1)
Z	phase-averaged sea level	(5.13)
$\mathscr{Z}$	rescaled vertical coordinate	after (3.1)
β	current/wave length-scale ratio	before (4.1)
γ	current/wave time-scale ratio	before (4.1)
$\Gamma[\cdot]$	differential operator	(5.8)
δ	current/wave horizontal velocity ratio	(4.1)
ϵ	wave slope parameter	§ 1
ζ	current sea-level elevation	(4.1)
$\zeta^c, \hat{\zeta}$	components of current sea level	(9.1)
η	wave sea-level elevation	(4.1)
η^{lw}	long-wave sea-level elevation	(4.1)
$\hat{\eta}^{lw}, \tilde{\eta}^{lw}$	components of η^{lw}	(6.3) *et seq.*
Θ	amplitude phase function	(5.36)
λ	long wave amplitude parameter	(4.1)
μ	wave depth parameter	before (2.1)
ν	wave/current ratio for materials	(10.2)
$\boldsymbol{\xi}^w$	wave horizontal vorticity	(7.1)
$\boldsymbol{\xi}^{lw}$	long-wave horizontal vorticity	(6.11)
$\hat{\boldsymbol{\xi}}^w$	wave horizontal vorticity component	(C 4)
$\hat{\hat{\boldsymbol{\xi}}}^w$	wave horizontal vorticity component	(C 5)
$\boldsymbol{\xi}^c$	current horizontal vorticity	(7.1)
Π	potential vorticity of depth-uniform currents	(12.2)
ρ	density	before (11.1)
ρ_0	mean density	before (2.1)
σ	wave frequency	(3.2)
Σ	dispersion relation	(5.20)
τ	slow wave time coordinate	(4.1)
Φ, ϕ	wave velocity potential	(3.3), (5.1)

TABLE 1. *Continued*

Symbol	Name	Where defined
φ^{lw}	horizontally divergent component of $\boldsymbol{q}^{lw}$	(6.5)
φ	horizontally divergent component of $\boldsymbol{v}$	(13.1)
χ^{w}	wave vertical vorticity	(7.1)
χ^{lw}	long-wave vertical vorticity	(6.11)
$\hat{\chi}^{w}$	wave vertical vorticity component	(C 4)
$\hat{\hat{\chi}}^{w}$	wave vertical vorticity component	(C 5)
χ^{c}	current vertical vorticity	(7.1)
ψ	vertically rotational component of $\boldsymbol{v}$	(13.1)
Ψ	combined current and Stokes-drift transport streamfunction	(12.5)
$\boldsymbol{\omega}^{c}$	current vorticity	(4.1)
$\boldsymbol{\omega}^{lw}$	long-wave vorticity	(4.1)
$\boldsymbol{\omega}^{w}$	wave vorticity	(4.1)
$\boldsymbol{\Omega}$	total 3D vorticity	before (2.1)
∇	3D spatial derivative	before (2.1)
∇_x	wave-scale horizontal derivative	before (2.1)
∇_X	slow horizontal derivative	after (4.1)
$\langle\cdot\rangle$, $\overline{(\cdot)}$	averages	before (4.2)
$(\cdot)'$, $(\cdot)^{\dagger}$	fluctuations	(4.2)

TABLE 1. *Continued*

REFERENCES

BENJAMIN, T. B. 1967 Instability of perioid wavetrains in nonlinear dispersive waves. *Proc. R. Soc. Lond.* **A 299**, 59–75.

BURROWS, R. & HEDGES, T. S. 1985 The influence of currents on ocean wave climates. *Coastal Engng* **9**, 247–260.

CHU, V. C. & MEI, C. C. 1970 On slowly varying Stokes waves. *J. Fluid Mech.* **41**, 873–887.

CRAIK, A. D. D. 1985 *Wave Interactions and Fluid Flows.* Cambridge University Press.

CRAIK, A. D. D. & LEIBOVICH, S. 1976 A rational model for Langmuir circulations. *J. Fluid Mech.* **73**, 401–426.

FENTON, J. D. 1990 Nonlinear wave theories. In *The Sea* (ed. B. LeMehaute & D. Hanes), vol. **9**(A), pp. 3–25). J. Wiley and Sons.

GRANT, W. & MADSEN, O. 1979 Combined wave and current interaction with a rough bottom. *J. Geophys. Res.* **84**, 1797–1808.

HIGDON, R. 1986 Absorbing boundary conditions for the wave equation. *Math. Comput.* **47**, 437–459.

HIGDON, R. 1987 Radiation boundary conditions for dispersive waves. *SIAM J. Numer. Anal.* **31**, 64–100.

ISAACSON, E. & KELLER, H. B. 1994 *Analysis of Numerical Methods* p. 541. Dover.

JONSSON, I. G. 1990 Wave-current interactions. In *The Sea* (ed. B. LeMehaute & D. Hanes), vol. **9**(A), 65–120. J. Wiley and Sons.

KELLER, J. 1958 Surface waves on water of non-uniform depth. *J. Fluid Mech.* **4**, 607–614.

KOMEN, G. J., CAVALERI, L., DONELAN, M., HASSELMANN, K., HASSELMANN, S. & JANSSEN, P. A. E. M. 1994 *Dynamics and Modelling of Ocean Waves.* Cambridge University Press.

LIGHTHILL, M. J. 1978 *Waves in Fluids.* Cambridge University Press.

LONGUET-HIGGINS, M. S. 1953 Mass transport in water waves. *Phil. Trans. R. Soc. Lond.* A **245**, 535–581.

LONGUET-HIGGINS, M. S. 1970 Longshore currents generated by obliquely incident sea waves, I. *J. Geophys. Res.* **75**, 6778–6789.

LONGUET-HIGGINS, M. S. & STEWART, R. W. 1960 Changes in the form of short gravity waves on long waves and tidal currents. *J. Fluid Mech.* **8**, 565–583.

LONGUET-HIGGINS, M. S. & STEWART, R. W. 1961 The changes in amplitude of short gravity waves on steady non-uniform currents. *J. Fluid Mech.* **10**, 529–549.

Longuet-Higgins, M. S. & Stewart, R. W. 1962 Radiation stress and mass transport in gravity waves, with applications to surf beats. *J. Fluid Mech.* **13**, 481–504.

Longuet-Higgins, M. S. & Stewart, R. W. 1964 Radiation stresses in water waves: A physical discussion with applications. *Deep-Sea Res.* **11**, 529–562.

McIntyre, M. E. 1981 On the "wave momentum" myth. *J. Fluid Mech.* **106**, 331–347.

McWilliams, J. C. & Flierl, G. R. 1979 On the evolution of isolated non-linear vortices. *J. Phys. Ocean ogr.* **9**, 1155–1182.

McWilliams, J. C. & Restrepo, J. M. 1999 The wave-driven ocean circulation. *J. Phys. Ocean ogr.* **29**, 2523–2540.

McWilliams, J. C., Sullivan, P. P., & Moeng, C.-H. 1997 Langmuir turbulence in the ocean. *J. Fluid Mech.* **334**, 1–30.

Mei, C. C. 1989 *The Applied Dynamics of Ocean Surface Waves.* World Scientific.

Mei, C. C. & Chian, C. 1994 Dispersion of suspended particles in wave boundary layers. *J. Phys. Ocean ogr.* **24**, 2479–2495.

Peregrine, H. 1967 Long waves on a beach. *J. Fluid Mech.* **27**, 815–827.

Peregrine, H. 1976 Interaction of water waves and currents. *Adv. Appl Mech.* **16**, 9–117.

Peregrine, H. & Thomas, G. 1979 Finite amplitude deep-water waves and currents. *Phil. Trans. R. Soc. Lond.* A, **292**, 371–390.

Prandle, D. 1997 The influence of bed friction and vertical eddy viscosity on tidal propagation. *Cont. Shelf. Res.* **17**, 1367–1374.

Restrepo, J. M. 2001 Sediment dynamics and wave-current interactions. *Cont. Shelf Res.* **21**, 1331–1360.

Restrepo, J. M. & Bona, J. L. 1995 Model for the formation of longshore sand ridges on the continental shelf. *Nonlinearity* **8**, 781–820.

Restrepo, J. M. & Leaf, G. K. 2002 Wave-generated transport induced by ideal waves. *J. Phys. Ocean org.* **32**, 2334–2349.

Thomas, G. P. 1981 Wave-current interactions: an experimental and numerical study. Part 1. Linear waves. *J. Fluid. Mech.* **110**, 457–474.

Thomas, G. P. 1990 Wave-current interactions: an experimental and numerical study. Part 2. Nonlinear waves. *J. Fluid. Mech.* **216**, 505-536.

Ursell, F. 1950 On the theoretical form of ocean swell on a rotating Earth. *Mon. Not. R. Astron. Soc. Geophys. Supplement* **6**, 1–8.

Wolf, J. & Prandle, D. 1999 Some observations of wave-current interaction. *Coastal Engng.* **37**, 471–485.

Yoon, S. B. & Liu, L. F. 1989 Interaction of currents and weakly nonlinear waters waves in shallow water. *J. Fluid. Mech.* **205**, 397–419.